

**EVALUATION OF FISSION PRODUCT CRITICAL EXPERIMENTS AND ASSOCIATED BIASES FOR BURNUP CREDIT VALIDATION**

Donald E. Mueller, Bradley T. Rearden and Davis A. Reed

*Oak Ridge National Laboratory<sup>1</sup>  
Nuclear Science and Technology Division  
P.O. Box 2008, Bldg. 5700  
Oak Ridge, TN 37831-6170 USA  
E-mail: muellerde@ornl.gov*

**Abstract** – One of the challenges associated with implementation of burnup credit is the validation of criticality calculations used in the safety evaluation; in particular the availability and use of applicable critical experiment data. The purpose of the validation is to quantify the relationship between reality and calculated results. Validation and determination of bias and bias uncertainty require the identification of sets of critical experiments that are similar to the criticality safety models. A principal challenge for crediting fission products (FP) in a burnup credit safety evaluation is the limited availability of relevant FP critical experiments for bias and bias uncertainty determination. This paper provides an evaluation of the available critical experiments that include FPs, along with bounding, burnup-dependent estimates of FP biases generated by combining energy dependent sensitivity data for a typical burnup credit application with the nuclear data uncertainty information distributed with SCALE 6. A method for determining separate bias and bias uncertainty values for individual FPs and illustrative results is presented. Finally, a FP bias calculation method based on data adjustment techniques and reactivity sensitivity coefficients calculated with the SCALE sensitivity/uncertainty tools and some typical results is presented. Using the methods described in this paper, the cross-section bias for a representative high-capacity spent fuel cask associated with the ENDF/B-VII nuclear data for 16 most important stable or near stable FPs is predicted to be no greater than 2% of the total worth of the 16 FPs, or less than 0.13 %  $\Delta k/k$ .

---

<sup>1</sup> This manuscript has been authored by UT-Battelle LLC under Contract No. DE-AC05-00OR22725 with the U.S. Department of Energy. The United States Government retains and the publisher, by accepting the article for publication, acknowledges that the United States Government retains a non-exclusive, paid-up, irrevocable, world-wide license to publish or reproduce the published form of this manuscript, or allow others to do so, for United States Government purposes.

## INTRODUCTION

Burnup credit is the analytical approach used to take credit in safety analyses for the reduction in reactivity of nuclear fuel that occurs during use in a power reactor. Burnup credit (BUC) results from depletion of  $^{235}\text{U}$  and in-growth of parasitic neutron absorbers that include non-fissile actinides and fission products (FPs). BUC is partially offset by the in-growth of some fissile nuclides such as  $^{239}\text{Pu}$  and  $^{241}\text{Pu}$ . The alternative to BUC is to assume that the fuel composition is in its fresh unirradiated state. The economic and safety-related benefits of BUC are documented in numerous studies [1, 2, 3, 4, 5, 6, 7].

American National Standards Institute (ANSI) American Nuclear Society (ANS) standard ANSI/ANS-8.24-2007, "Validation of Neutron Transport Methods for Nuclear Criticality Safety Calculations," [8] provides guidance and recommendations applicable to the validation of computational methods. ANSI/ANS-8.27-2008, "Burnup Credit for LWR Fuel," [9] provides guidance and recommendations specific to validation of computations used to support BUC. One of the purposes of validation is establish a quantitative relationship between calculated values and reality. Typically, this is accomplished by using the computational method, which is defined as the combination of computer hardware, programs, data, and modeling processes being validated, to model physical systems for which a computational result has been measured. The variation between the calculated and measured results is characterized by the bias and bias uncertainty.

BUC validation has two aspects, which ANSI/ANS-8.27 says may be evaluated either together or separately. The first component is related to the computational method's ability to calculate the used or "burned" fuel composition. The second aspect is related to the computational method's ability to calculate the system neutron multiplication factor ( $k_{eff}$ ) for a system containing burned fuel compositions. This paper does not address validation of the fuel composition calculations. It is instead focused solely on validation of  $k_{eff}$  calculations and, more specifically, on  $k_{eff}$  calculations for systems containing FPs. This paper includes a description of the computational methods used in the reported work, a description of a representative burnup credit safety analysis model, cross-section uncertainty analysis for the safety analysis model, a description of the critical experiment data available for validation of FPs, and some discussion of how the SCALE sensitivity/uncertainty (S/U) analysis tools may be used to calculate nuclide-specific biases for FPs present in the safety analysis model.

## BURNUP CREDIT ANALYSIS AND VALIDATION

Typically,  $k_{eff}$  calculation validation involves modeling critical configurations that are similar to the safety analysis case or cases and performing statistical analysis of the results to produce a bias and bias uncertainty applicable to the safety analysis cases. The similarity of the critical experiments to the safety analysis (SA) models is important to ensure that the bias, determined from the critical experiments, is applicable to the SA model(s). For example, if there was a bias in the SA model due to errors in a particular material's cross section, but that material was not present in the critical experiments used to estimate the bias, the estimated bias would be erroneous. Similarly, significant differences in neutron energy spectra between the SA model and

the critical experiments could result in the determination of an erroneous bias. Accurate bias determination requires that the same nuclear data be used in the same fashion in both the SA models and the critical experiments. Historically, similarity has been left largely to the professional judgment of the engineers performing and reviewing the work. Frequently, parameters such as enrichment, solution concentration, H/fissile atom ratio, material form, neutron spectra comparisons, and energy of average lethargy of neutrons causing fission (EALF) were used to assess similarity. More recently, the SCALE S/U analysis tools, which provide a means for rigorous, physics-based assessment of similarity, have become available to the criticality safety community. The SCALE S/U tools were used in the work reported in this paper.

For fresh commercial spent nuclear fuel (CSNF), the fuel composition is low-enriched UO<sub>2</sub>, for which a large number of applicable critical experiments are widely available. This is not the case for validation of calculations involving burned fuel compositions that include neptunium (<sup>237</sup>Np), plutonium (<sup>238</sup>Pu, <sup>239</sup>Pu, <sup>240</sup>Pu, <sup>241</sup>Pu, and <sup>242</sup>Pu), americium (<sup>241</sup>Am and <sup>243</sup>Am), and FPs such as <sup>95</sup>Mo, <sup>99</sup>Tc, <sup>101</sup>Ru, <sup>103</sup>Rh, <sup>109</sup>Ag, <sup>133</sup>Cs, <sup>143</sup>Nd, <sup>145</sup>Nd, <sup>147</sup>Sm, <sup>149</sup>Sm, <sup>150</sup>Sm, <sup>151</sup>Sm, <sup>152</sup>Sm, <sup>151</sup>Eu, <sup>153</sup>Eu, and <sup>155</sup>Gd.

## COMPUTATIONAL METHODS

The computational work presented in this paper was performed using the following SCALE 6 [10] sequences, modules and nuclear data:

- CSAS5 and CSAS6 sequences were used to perform standard Monte Carlo  $k_{eff}$  calculations for critical experiments and for the safety applications;
- STARBUCS sequence was used to calculate burned fuel compositions for initial <sup>235</sup>U enrichment and burnup pairs along a typical burnup credit loading curve;
- TSUNAMI-3D sequence was used to generate nuclide-, energy-, and reaction-dependent  $k_{eff}$  sensitivity data;
- TSUNAMI-IP module was used to combine the  $k_{eff}$  sensitivity data with the cross-section uncertainty data distributed with SCALE 6 to calculate the uncertainty in the  $k_{eff}$  values due to cross-section uncertainties;
- TSAR module was used to calculate reactivity sensitivities based on critical configurations with and without FPs;
- TSURFER module was used to estimate FP biases using a generalized linear least-squares technique, sometimes called data adjustment;
- 238-neutron-energy-group ENDF-B-VII library and 44-group covariance data library were used as needed in the various sequences and modules;
- Javapeño data display program was used to prepare sensitivity and cross-section uncertainty plots; and
- KENO3D program was used to generate the figures of the SA and the laboratory critical experiment (LCE) models.

Additional details on the computational methods used are provided within the relevant sections of this paper.

## REPRESENTATIVE BURNUP CREDIT ANALYSIS MODEL (GBC-32)

A representative 32 pressurized water reactor (PWR) fuel assembly transportation cask, referred to as the GBC-32 [11], was used as the SA model in this study. The GBC-32 model, shown in Figure 1, includes 32 Westinghouse  $17 \times 17$  optimized fuel assemblies (OFAs). Assembly average burnup values ranging from 5 to 50 GWd/MTU were considered in this study, and the fuel was modeled using 18 axial burnup zones. The SCALE STARBUCS sequence was used to calculate loading curves (target  $k_{eff}$  of 0.94) for two sets of fuel isotopic compositions. The first set is referred to as “Major Actinides Only” and includes  $^{234}\text{U}$ ,  $^{235}\text{U}$ ,  $^{238}\text{U}$ ,  $^{238}\text{Pu}$ ,  $^{239}\text{Pu}$ ,  $^{240}\text{Pu}$ ,  $^{241}\text{Pu}$ ,  $^{242}\text{Pu}$ , and  $^{241}\text{Am}$ . The second set is referred to as “Actinides & 16 FP” and included these same nuclides and actinides  $^{236}\text{U}$ ,  $^{237}\text{Np}$ ,  $^{243}\text{Am}$ , and FPs  $^{95}\text{Mo}$ ,  $^{99}\text{Tc}$ ,  $^{101}\text{Ru}$ ,  $^{103}\text{Rh}$ ,  $^{109}\text{Ag}$ ,  $^{133}\text{Cs}$ ,  $^{147}\text{Sm}$ ,  $^{149}\text{Sm}$ ,  $^{150}\text{Sm}$ ,  $^{151}\text{Sm}$ ,  $^{152}\text{Sm}$ ,  $^{143}\text{Nd}$ ,  $^{145}\text{Nd}$ ,  $^{151}\text{Eu}$ ,  $^{153}\text{Eu}$ , and  $^{155}\text{Gd}$ . Note that no corrections were made to the calculated fuel compositions to account for bias and bias uncertainty in the isotopic composition predictions (i.e., isotopic validation). The fuel composition calculations assumed that wet annular burnable absorber (WABA) rods were present throughout the fuel depletion and that the fuel underwent a 5-year post-irradiation cooling period. Each fuel assembly sits in a stainless steel cell with one BORAL™ plate between each assembly and on the outside of each peripheral location. The cask has a thick stainless steel body and lid and is modeled as if flooded with water.

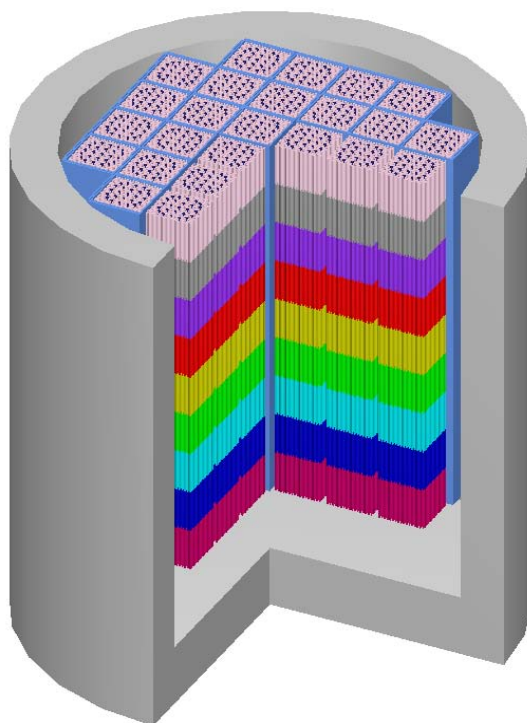


Figure 1. Cut-away view of the generic burnup credit cask (GBC-32) model

Figure 2 shows the Major Actinide and Actinides & 16 FP loading curves superimposed on the inventory of Westinghouse  $17 \times 17$  assemblies stored at reactor sites as of the end of 2002 [12]. The point of the figure is to illustrate the potential value of taking credit for FPs. Including credit for FPs and minor actinides significantly increases the inventory of assemblies that could be loaded into this cask and significantly decreases the inventory of assemblies that represent potential misloads for this cask (note: assemblies below the governing loading curve, which are not acceptable for loading, are assemblies that could potentially be mistakenly loaded into a cask).

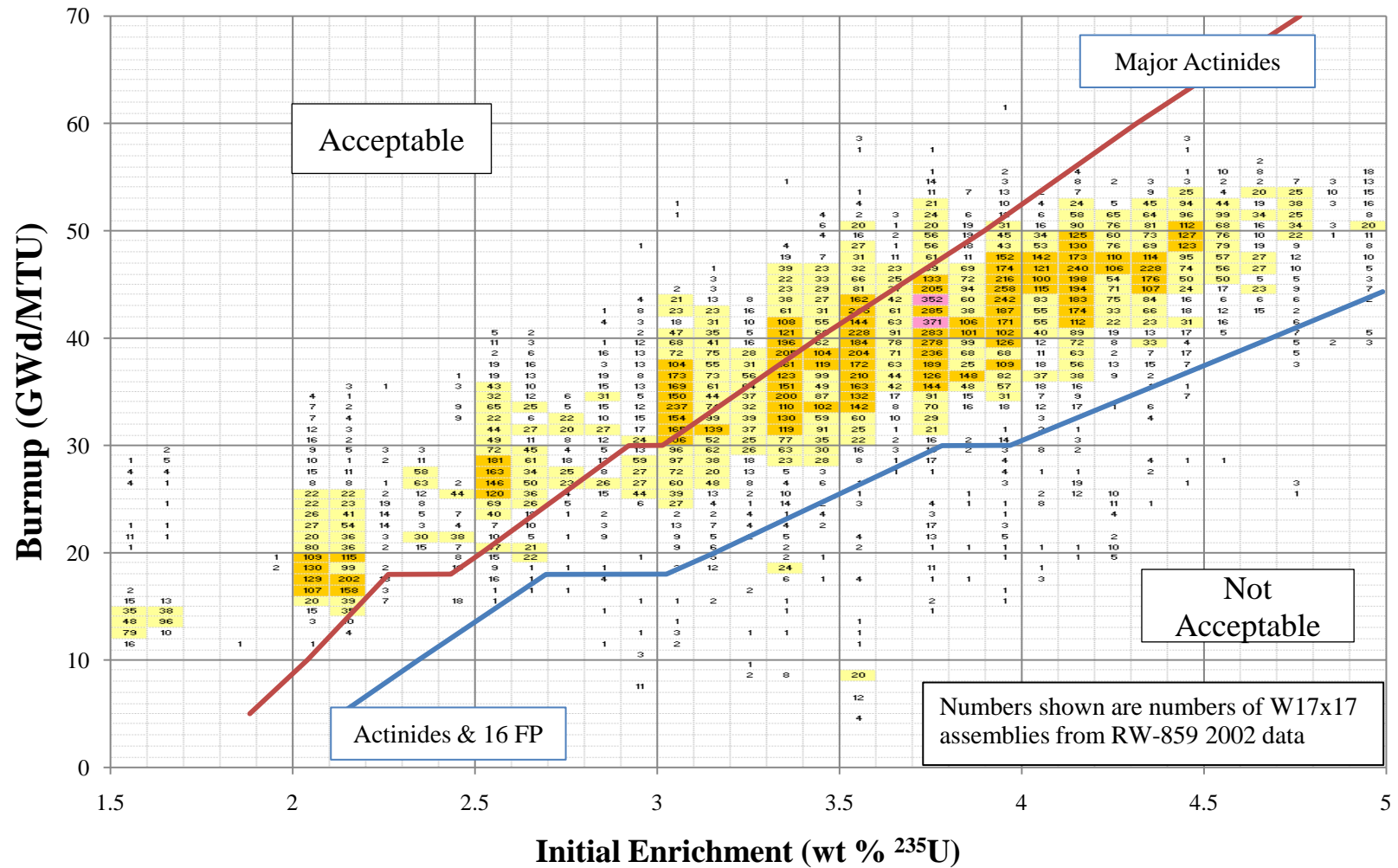


Figure 2. GBC-32 burnup credit loading curves for Westinghouse (W) 17 × 17 fuel assemblies superimposed onto the discharged inventory of W 17 × 17 fuel assemblies as of 2002

### GBC-32 SENSITIVITY ANALYSIS

The SCALE TSUNAMI-3D sequence was used to calculate the sensitivity of  $k_{eff}$  to the nuclide-, energy-, and reaction-dependent multi-group cross-section data for the GBC-32 cask model loaded with fuel that had initial enrichments and final burnup values consistent with the Actinide & 16 FP loading curve show in Figure 2. The sensitivity values represent the fractional change in the system  $k_{eff}$  that would result from a fractional change in the nuclear data parameter of interest. The sensitivity values are based on linear perturbation theory and forward and adjoint Monte Carlo criticality (i.e., KENO) calculations. The TSUNAMI sensitivity calculations include both an explicit component resulting from how nuclear data directly affects the transport calculation and an implicit component resulting from how the presence of a nuclide affects the resonance self-shielding calculations associated with multi-group cross sections [13]. A sensitivity value of -0.5 means a 1% increase in the nuclear data value will cause a 0.5% decrease in  $k_{eff}$ .

Figures 3 through 8 provide information on the burnup-dependent behavior of some key nuclides and reactions in the GBC-32 cask model. Figures 3 through 5 show the shift of fissions from  $^{235}\text{U}$  to  $^{239}\text{Pu}$  and  $^{241}\text{Pu}$ , respectively. Note from Figure 4 that the  $^{239}\text{Pu}$  has grown to a near-equilibrium level by 20 GWd/MTU.

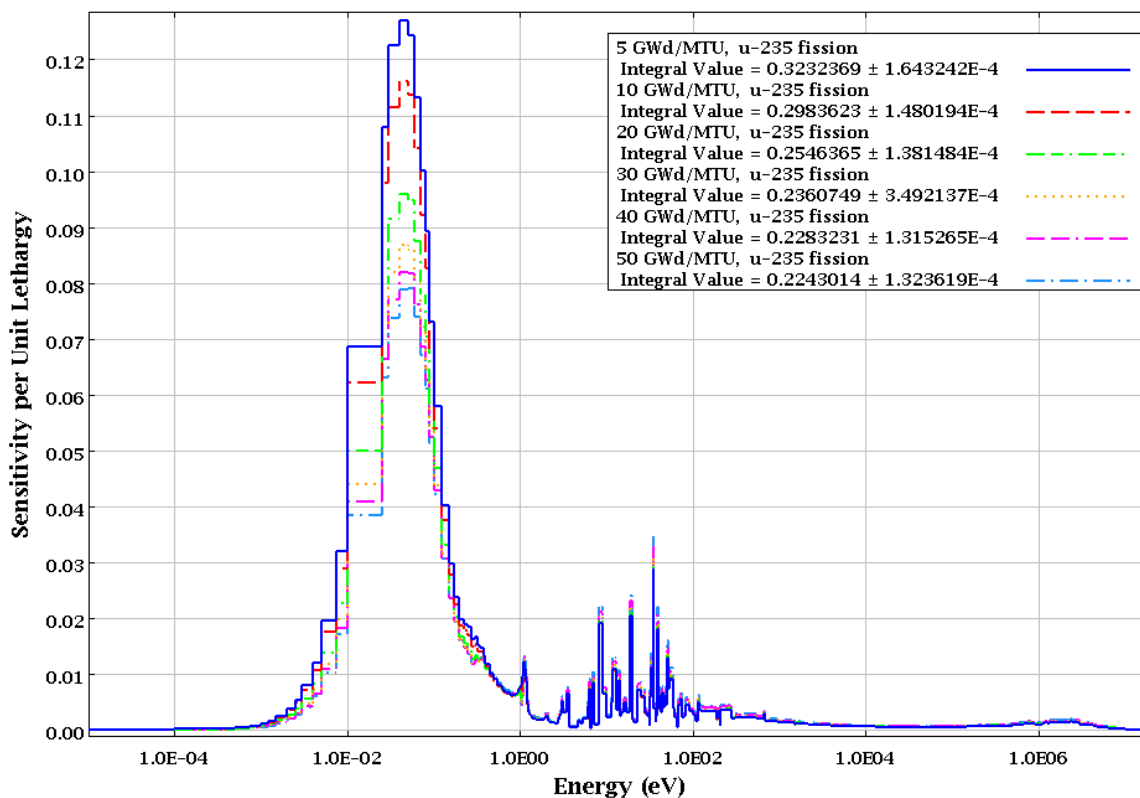


Figure 3. GBC-32  $^{235}\text{U}$  fission sensitivity as a function of assembly average burnup

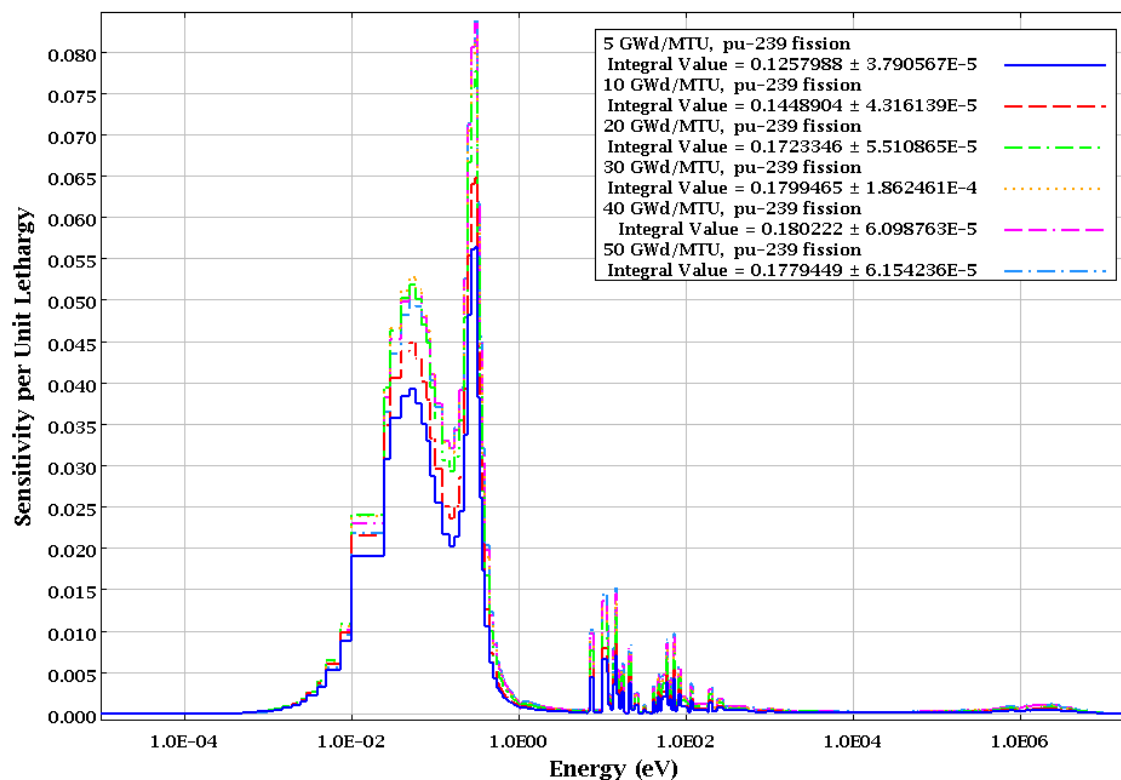


Figure 4. GBC-32 <sup>239</sup>Pu fission sensitivity as a function of assembly average burnup

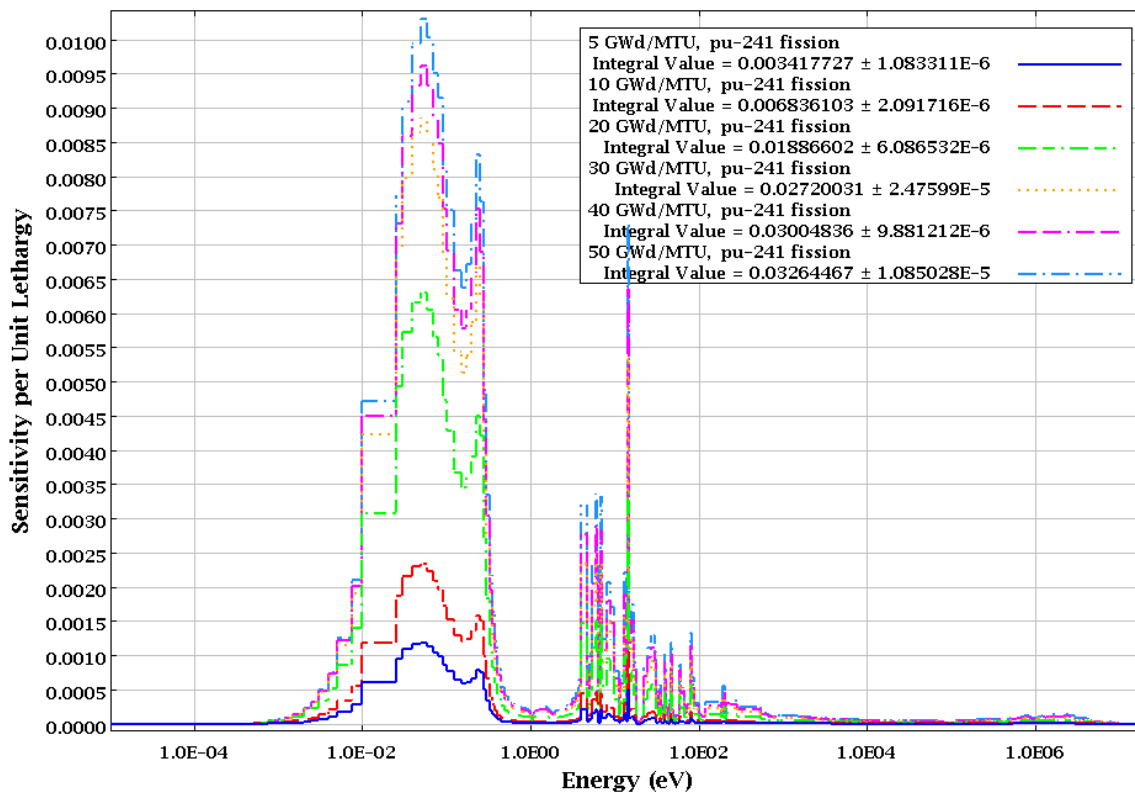
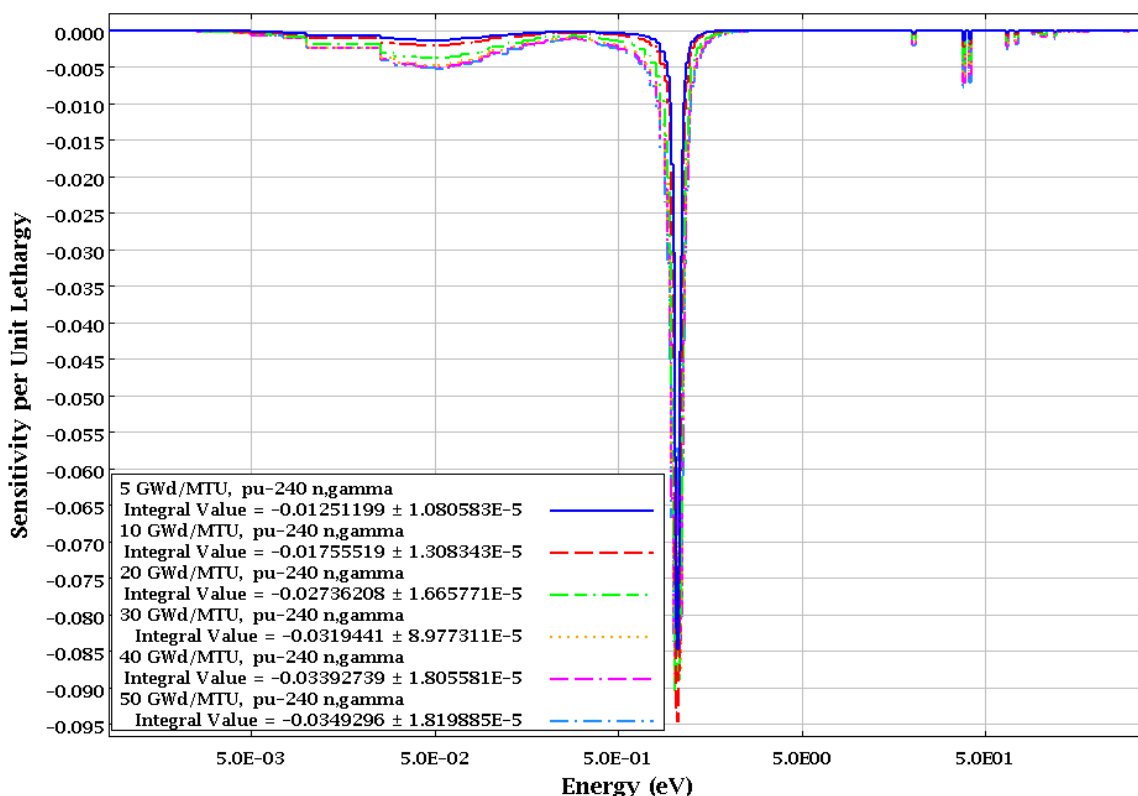


Figure 5. GBC-32 <sup>241</sup>Pu fission sensitivity as a function of assembly average burnup

Figure 6 shows the in-growth of  $^{240}\text{Pu}$ , which is a major neutron absorber.



**Figure 6. GBC-32  $^{240}\text{Pu}$  n,gamma sensitivity as a function of assembly average burnup**

Figure 7 shows the burnup dependence of the sensitivity of  $^{149}\text{Sm}$ , which is the stable FP with the largest reactivity worth in typical spent fuel systems. This FP is somewhat unique in that it reaches its equilibrium worth relatively quickly as compared to the other FPs that might be credited in BUC analysis. Figure 8 shows the burnup dependence of  $^{143}\text{Nd}$ , which is the stable FP with the second largest reactivity worth in typical spent fuel systems. Note that its sensitivity increases throughout the burnup range examined. This behavior is generally representative of the major FPs that are relevant to BUC analysis.

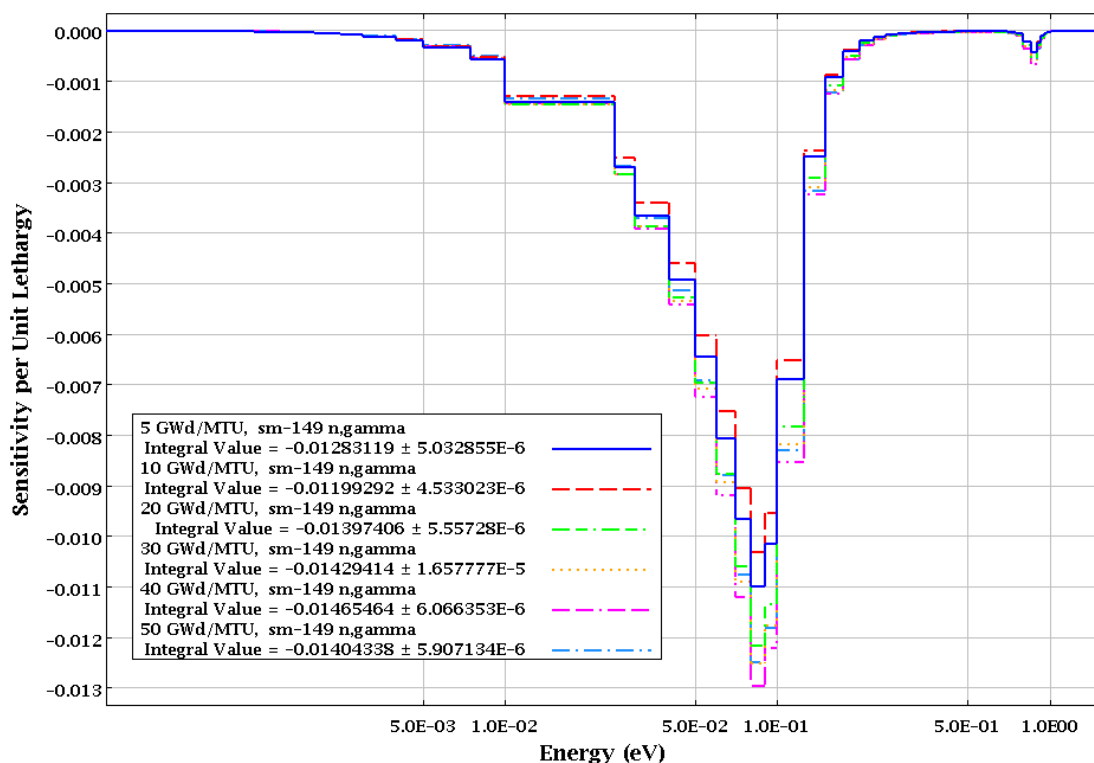


Figure 7. GBC-32  $^{149}\text{Sm}$  n, $\gamma$  sensitivity as a function of assembly average burnup

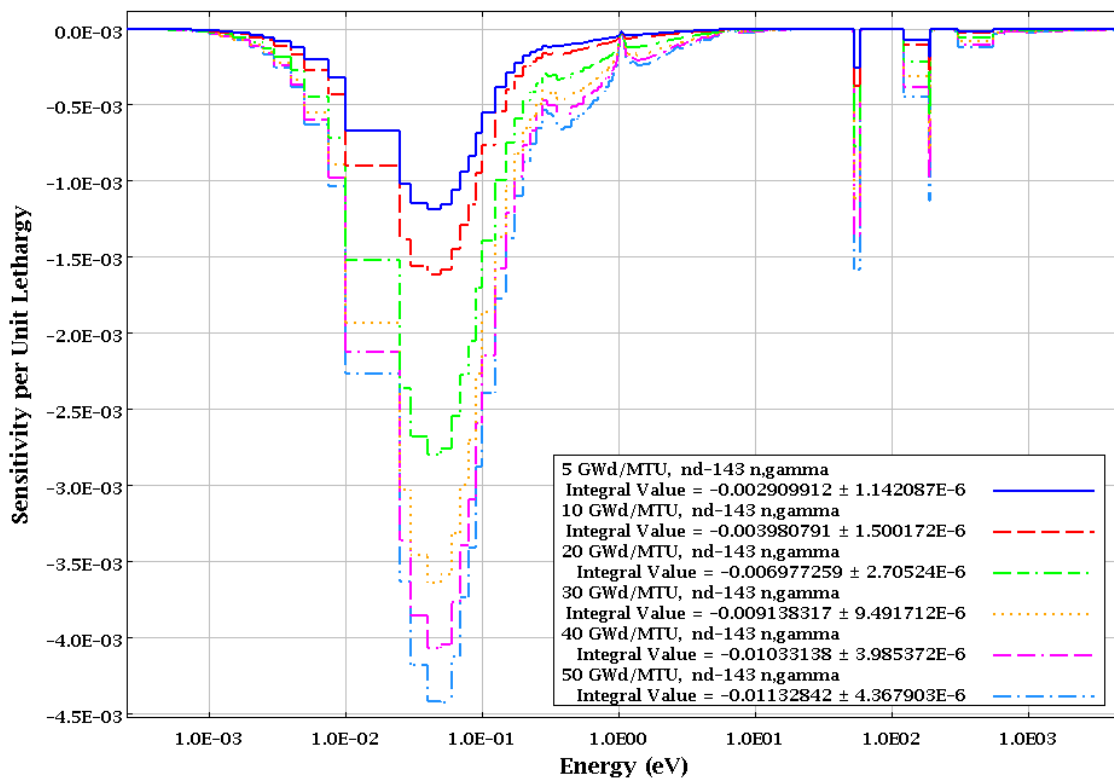


Figure 8. GBC-32  $^{143}\text{Nd}$  n, $\gamma$  sensitivity as a function of assembly average burnup

Figure 9 shows the burnup dependent behavior of the reactivity worth of the top 16 stable or near stable FPs in the GBC-32 cask. The total reactivity worth of these 16 FPs increases from about 2.5%  $\Delta k/k$  at 5 GWd/MTU to nearly 7%  $\Delta k/k$  at 50 GWd/MTU. Note that these FP reactivity worth values are based on as-calculated isotopic compositions (i.e., no adjustments for isotopic composition bias and uncertainty).

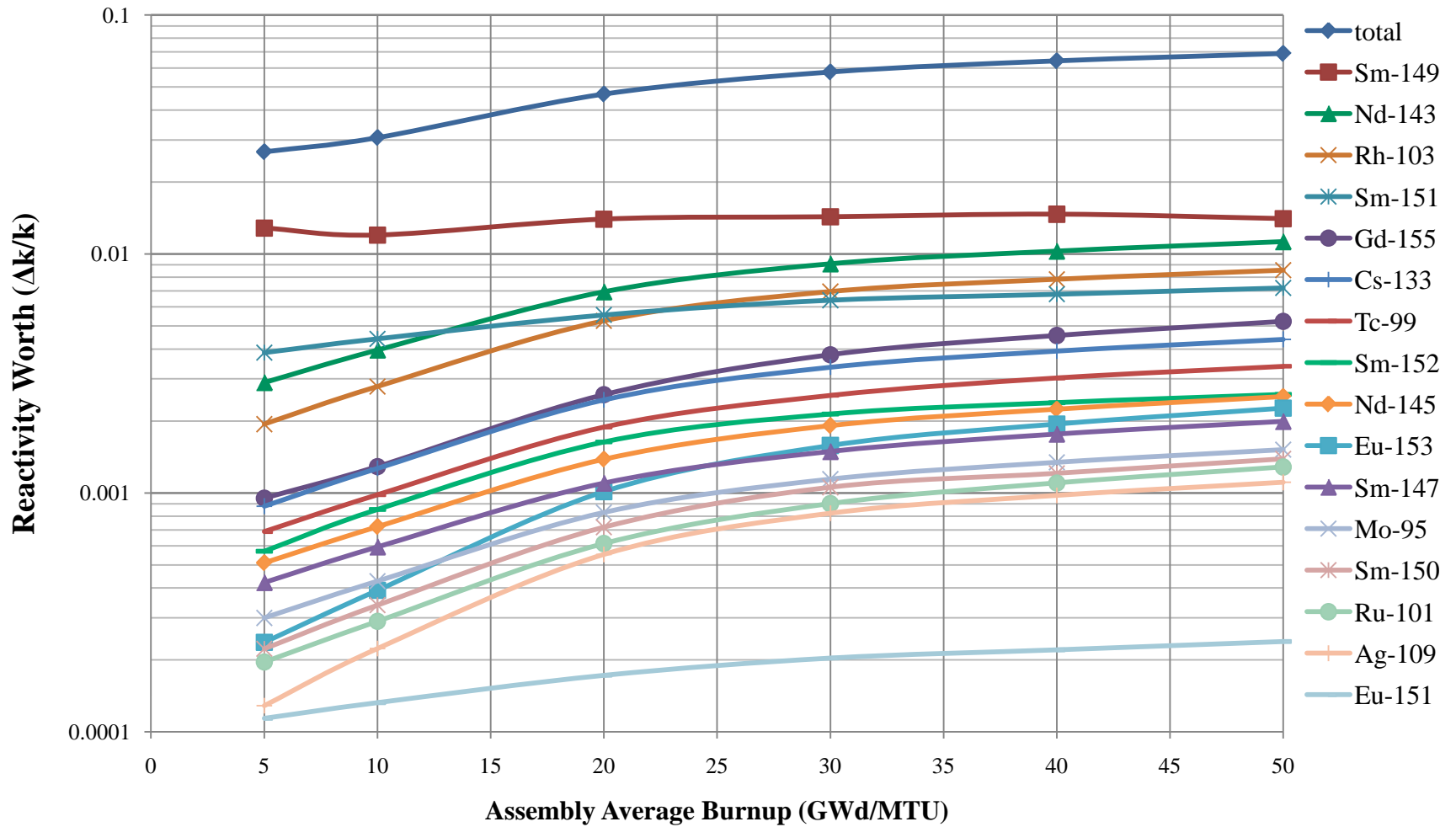


Figure 9. Reactivity worth of FPs in GBC-32 as a function of burnup

## GBC-32 UNCERTAINTY ANALYSIS

The SCALE TSUNAMI-IP module was used to combine the burnup-dependent sensitivity data with the nuclear data uncertainty information contained in the cross-section covariance data file distributed with SCALE 6 to generate uncertainties in the GBC-32 model  $k_{eff}$  value due to cross-section uncertainties. The mathematics associated with these calculations are described in Section F22.2.5 of the SCALE 6 manual [10]. Figure 10 and Table 1 show the burnup-dependent uncertainty analysis results for the GBC-32 cask model.

The highest curve in this figure is the uncertainty in  $k_{eff}$  due to all nuclear data uncertainties. For this model, the one-standard-deviation ( $1\sigma$ ) uncertainty in  $k_{eff}$  due to nuclear data uncertainties associated with all materials in the cask model is fairly constant at around 0.5%  $\Delta k/k$  for the entire burnup range. Thus one does not expect to observe a bias greater than  $\sim 1\%$   $\Delta k/k$ . A study by Rearden et al. documented in a manuscript under preparation for publication in Nuclear Technology shows a comparison of the differences between the expected and calculated  $k_{eff}$  values for each of 186 critical experiments, which include a variety of uranium, plutonium and mixed uranium-plutonium systems. The uncertainties in the calculated  $k_{eff}$  values due to cross-section-covariance data were also quantified for each critical experiment. For each case, its computational bias is bounded by two standard deviations of its nuclear data uncertainty, and in nearly all cases the bias in  $k_{eff}$  was bounded by one standard deviation. As can be seen from Figure 10 and Table 1, the combined uncertainty ( $1\sigma$ ) for the 16 modeled FPs for fuel assembly burnup values ranging from 5 to 50 GWd/MTU is less than 0.065 %  $\Delta k/k$ . Thus one would expect the combined biases for the 16 FPs to be less than the  $2\sigma$ -uncertainty value of 0.13%  $\Delta k/k$ .

Assuming the uncertainties associated with FP cross sections are uncorrelated, the total uncertainty in  $k_{eff}$  due to the 16 modeled FPs increases from one twentieth to about one-tenth of the total uncertainty as burnup increases from 5 to 50 GWd/MTU. Thus the biases caused by FP cross-section errors are predicted to be small compared to the overall bias applicable to the GBC-32 model. In general, the trends in Figure 10 are similar to the trends in Figure 9 with the primary difference being that the differences in the cross section uncertainties affect the order of the curves. For example, the uncertainty in the  $^{143}\text{Nd}$  cross sections at thermal and intermediate neutron energies is significantly greater than the uncertainty in the  $^{149}\text{Sm}$  cross sections (Figure 11). Consequently, even though  $^{149}\text{Sm}$  has a higher worth,  $^{143}\text{Nd}$  contributes more to uncertainty.

Figure 12 shows the total uncertainty due to FP cross sections divided by the total FP reactivity worth in the GBC-32 model. Note that over the range from 5 to 50 GWd/MTU the uncertainty in the total FP worth is less than 1%. Indeed, extrapolation of the burnup-dependent trend to 70 GWd/MTU would still be less than 1%. Consequently, it is unlikely that the bias associated with the 16 modeled FPs would be as great as 2% ( $2\sigma$ ) of the total FP worth in the GBC-32 model.

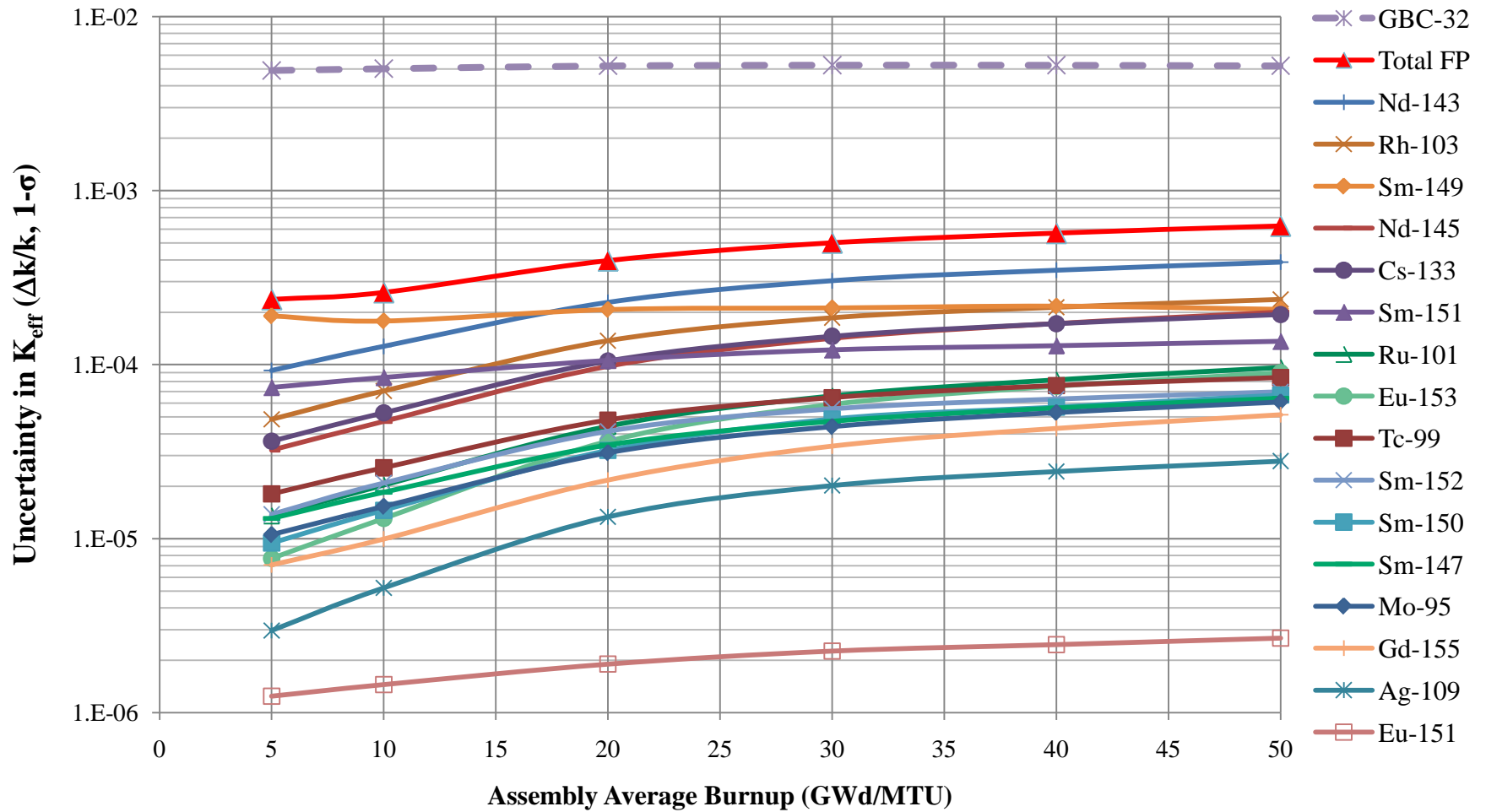


Figure 10. Uncertainty in GBC-32  $k_{eff}$  due to nuclear data uncertainties as a function of burnup

**Table 1. Uncertainty (%  $\Delta k/k$ ) in GBC-32  $k_{eff}$  due to FP Nuclear Data Uncertainties as a Function of Burnup**

	Assembly Average Burnup (GWd/MTU)					
	5	10	20	30	40	50
	Uncertainty in $k_{eff}$ (% $\Delta k/k$ )					
<sup>143</sup> Nd	0.0092	0.0127	0.0228	0.0304	0.0349	0.0388
<sup>103</sup> Rh	0.0049	0.0071	0.0137	0.0186	0.0214	0.0237
<sup>149</sup> Sm	0.0190	0.0178	0.0207	0.0212	0.0217	0.0208
<sup>145</sup> Nd	0.0032	0.0047	0.0098	0.0142	0.0172	0.0200
<sup>133</sup> Cs	0.0036	0.0053	0.0105	0.0145	0.0172	0.0194
<sup>151</sup> Sm	0.0074	0.0084	0.0106	0.0122	0.0129	0.0136
<sup>101</sup> Ru	0.0014	0.0020	0.0044	0.0066	0.0082	0.0096
<sup>153</sup> Eu	0.0008	0.0013	0.0036	0.0059	0.0075	0.0090
<sup>99</sup> Tc	0.0018	0.0026	0.0048	0.0065	0.0076	0.0084
<sup>152</sup> Sm	0.0014	0.0021	0.0041	0.0056	0.0063	0.0070
<sup>150</sup> Sm	0.0009	0.0015	0.0032	0.0049	0.0057	0.0067
<sup>147</sup> Sm	0.0013	0.0018	0.0035	0.0047	0.0056	0.0064
<sup>95</sup> Mo	0.0011	0.0015	0.0031	0.0044	0.0053	0.0061
<sup>155</sup> Gd	0.0007	0.0010	0.0022	0.0034	0.0043	0.0052
<sup>109</sup> Ag	0.0003	0.0005	0.0013	0.0020	0.0024	0.0028
<sup>151</sup> Eu	0.0001	0.0001	0.0002	0.0002	0.0002	0.0003
16 FP <sup>†</sup>	0.0237	0.0260	0.0396	0.0501	0.0569	0.0626
GBC-32*	0.4904	0.5018	0.5213	0.5264	0.5257	0.5214

<sup>†</sup> Combined quadratically assuming independent uncertainties.

\* Total uncertainty in  $k_{eff}$  due to nuclear data uncertainties for all materials in the GBC-32 cask model.

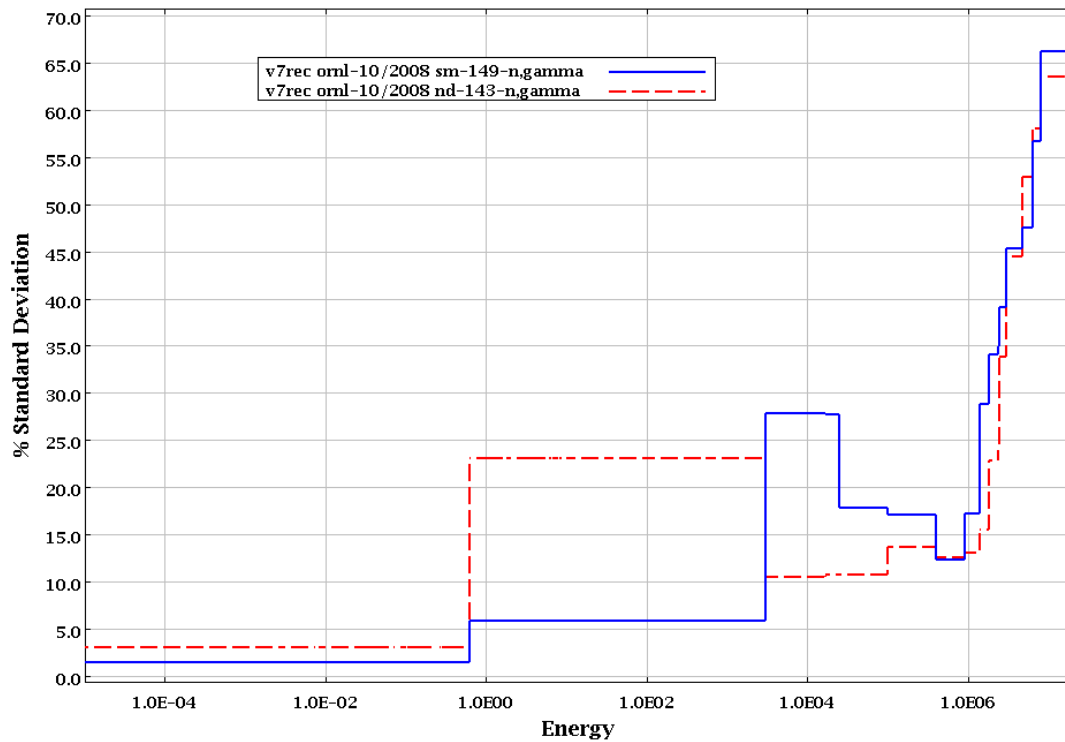


Figure 11. Uncertainty in n,γ capture cross sections for <sup>149</sup>Sm and <sup>143</sup>Nd

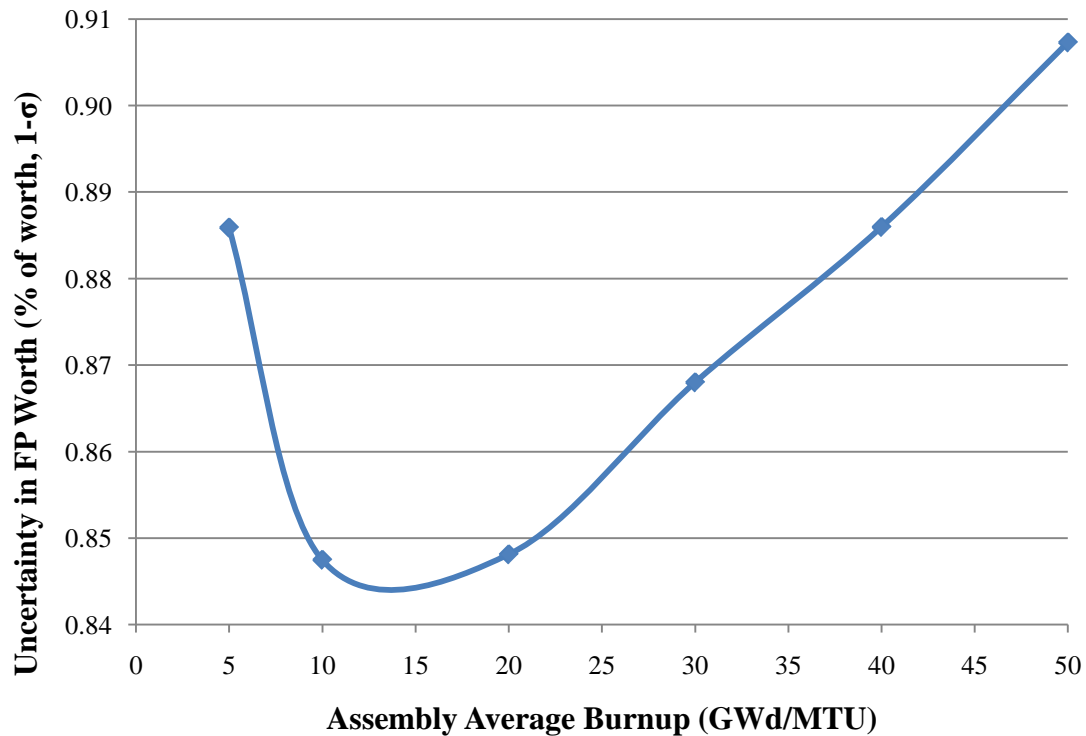


Figure 12. Uncertainty in total FP reactivity worth in GBC-32 due to nuclear data uncertainties as a function of burnup

## FP EXPERIMENTAL DATA

Conventional validation of BUC calculations that credit FPs requires well-characterized critical experiments that are similar to the SA model, which includes spent fuel with FPs. If the actinides and FPs were present in the proper proportions, a total overall bias could be quantified. Strictly speaking, there are no such experiments available.

Validation for actinide-only burnup credit is possible with the French Haut Taux de Chaux (HTC) critical experiment data [14, 15, 16, 17] and other U/Pu mixed-oxide (MOX) critical experiment data available in the *International Handbook of Evaluated Criticality Safety Benchmark Experiments* (IHECSBE) [18]. Due to the proprietary nature of the HTC data, specific details are not provided in this paper. The fissionable material actinide compositions in the HTC experiments were fabricated to be similar to spent fuel that had an initial  $^{235}\text{U}$  enrichment of 4.5 wt % and was burned to 37.5 GWd/MTU. An evaluation of the suitability of the HTC data for validation of actinide-only burnup credit calculations was documented in NUREG/CR-6979 [19]. The findings of that report indicate that the HTC data are useful for validating actinide-only burnup credit calculations for commercial PWR spent nuclear fuel (SNF) with burnup values of 20 GWd/MTU and higher in a high-capacity cask, similar to the GBC-32.

This section of the paper includes a brief review of the following available data that may be useful for validation of FP burnup credit.

- IHECSBE evaluation LEU-COMP-THERM-050 –  $^{149}\text{Sm}$  experiments
- IHECSBE evaluation LEU-COMP-THERM-079 –  $^{103}\text{Rh}$  experiments
- IHECSBE evaluation LEU-MISC-THERM-005 – FP element experiments
- IHECSBE evaluation HEU-COMP-INTER-005 – case 3 – Mo critical configuration
- IHECSBE experiments with natural gadolinium
- REBUS Program – spent fuel configurations
- MINERVE FP Reactivity Worth Measurements
- French FP Experiments
- Commercial Reactor Criticals (CRCs)

### ➤ LEU-COMP-THERM-050 – $^{149}\text{Sm}$ experiments

This IHECSBE evaluation documents 18 critical configurations that involve a Zircaloy tank in the middle of an array of Al clad U(4.738 wt %  $^{235}\text{U}$ )O<sub>2</sub> fuel rods. The tank is filled with water in two configurations, boron solution in five configurations, and samarium nitrate at one of three different samarium concentrations in 11 configurations. The array is in a large tank, in which the water level is adjusted to approach criticality. The samarium is enriched to 96.9 atom %  $^{149}\text{Sm}$ . Figure 13 is a KENO3D isometric view of one of the configurations with the right front corner removed. These experiments are part of a larger critical experiment program [20] and are similar

to the “physical experiments” described in Ref. 20. Modeling details for the 145 critical configurations documented as part of the FP Experimental Program are not publicly available.

Figure 14 shows the energy-dependent  $k_{eff}$  sensitivities to the  $^{149}\text{Sm}$  total macroscopic cross section in these critical configurations (red curves) along with the burnup-dependent  $^{149}\text{Sm}$  sensitivities from the GBC-32 cask model (green curves). Note that the two sets of sensitivity curves are fairly similar.

These experiments contain no plutonium and hence are not usable in “conventional” bias determination. Use of this data to quantify FP biases may still be possible, as is discussed later in the section on FP bias determination.

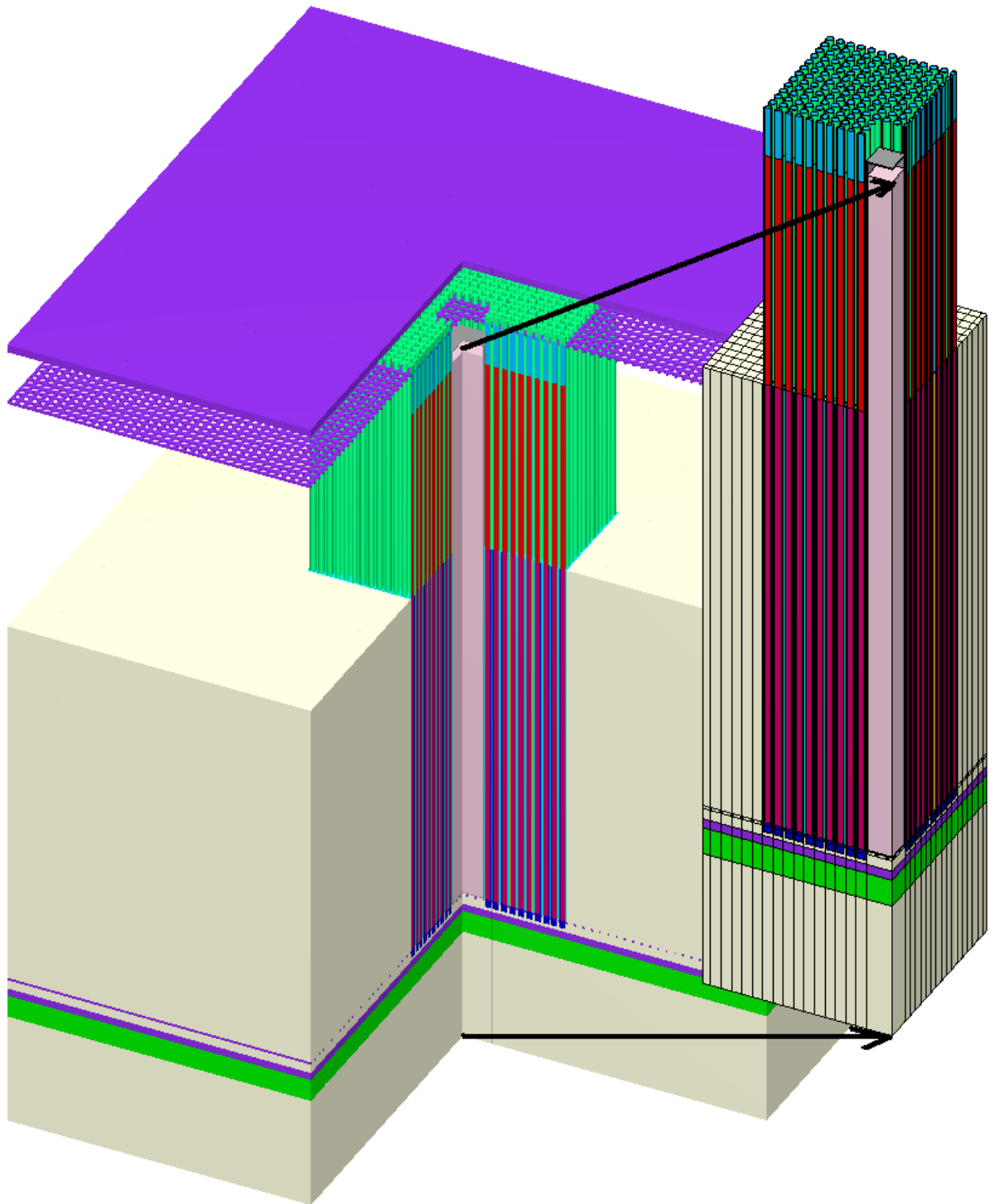


**Figure 13. LEU-COMP-THERM-050 critical configuration**

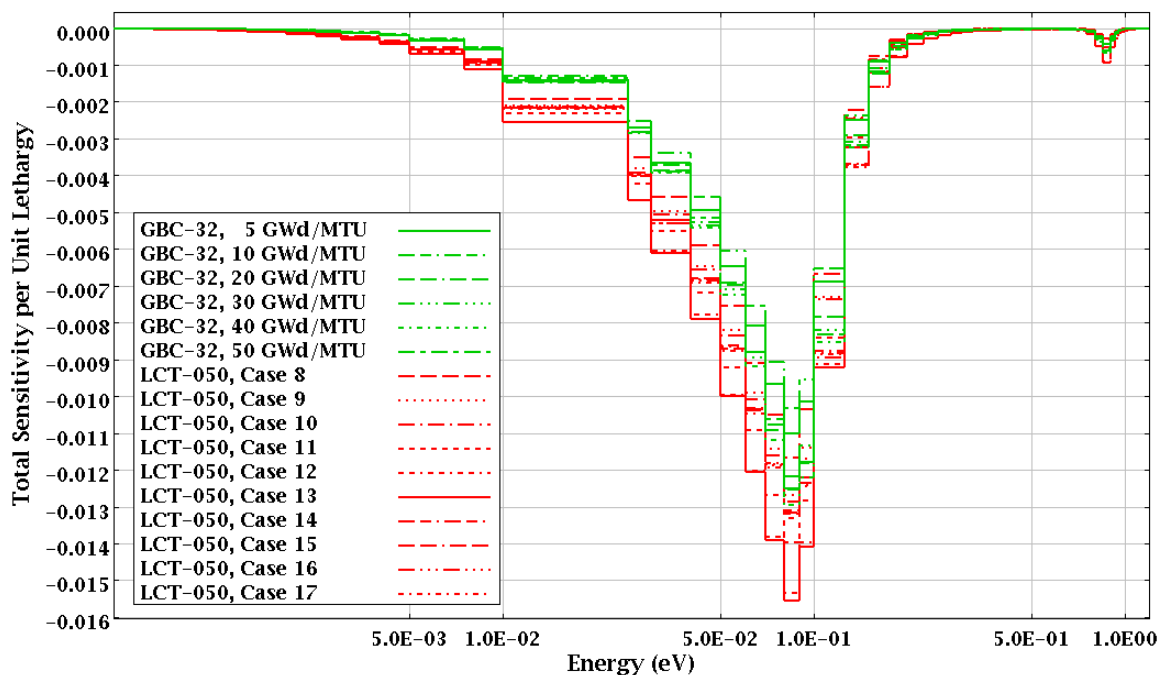


Figure 14. LEU-COMP-THERM-050 and GBC-32  $^{149}\text{Sm}$  sensitivity profiles

➤ LEU-COMP-THERM-079 –  $^{103}\text{Rh}$  experiments

This IHECSBE evaluation documents 10 critical configurations that involve a triangular-pitched array of Zircaloy clad  $\text{U}(4.31\%)\text{O}_2$  fuel elements. In six of the configurations, 25-, 50-, or 100-micron-thick  $^{103}\text{Rh}$  foils were placed between fuel pellets in 36 elements. Criticality was achieved by adding unpoisoned fuel elements to the outside of the water moderated and reflected array. Figure 15 is a KENO3D isometric view of one of the configurations with the right front quarter and the water-removed. Figure 16 shows the energy-dependent  $k_{eff}$  sensitivities to the  $^{103}\text{Rh}$  total macroscopic cross section in these critical configurations (red curves) along with the burnup-dependent  $^{103}\text{Rh}$  sensitivities from the GBC-32 cask model (green curves).

The sets of curves for LEU-COMP-THERM-079 are significantly different from the GBC-32 curves. As is discussed in Ref. 21, the differences just above 1 eV appear to be due to absorber lump self-shielding. Consequently, the potential impact of biases associated with the peak would be significantly underestimated using the critical configurations.

These experiments contain no plutonium and hence are not usable in “conventional” bias determination. Use of this data to quantify FP biases may still be possible, as is discussed later in the section on FP bias determination.

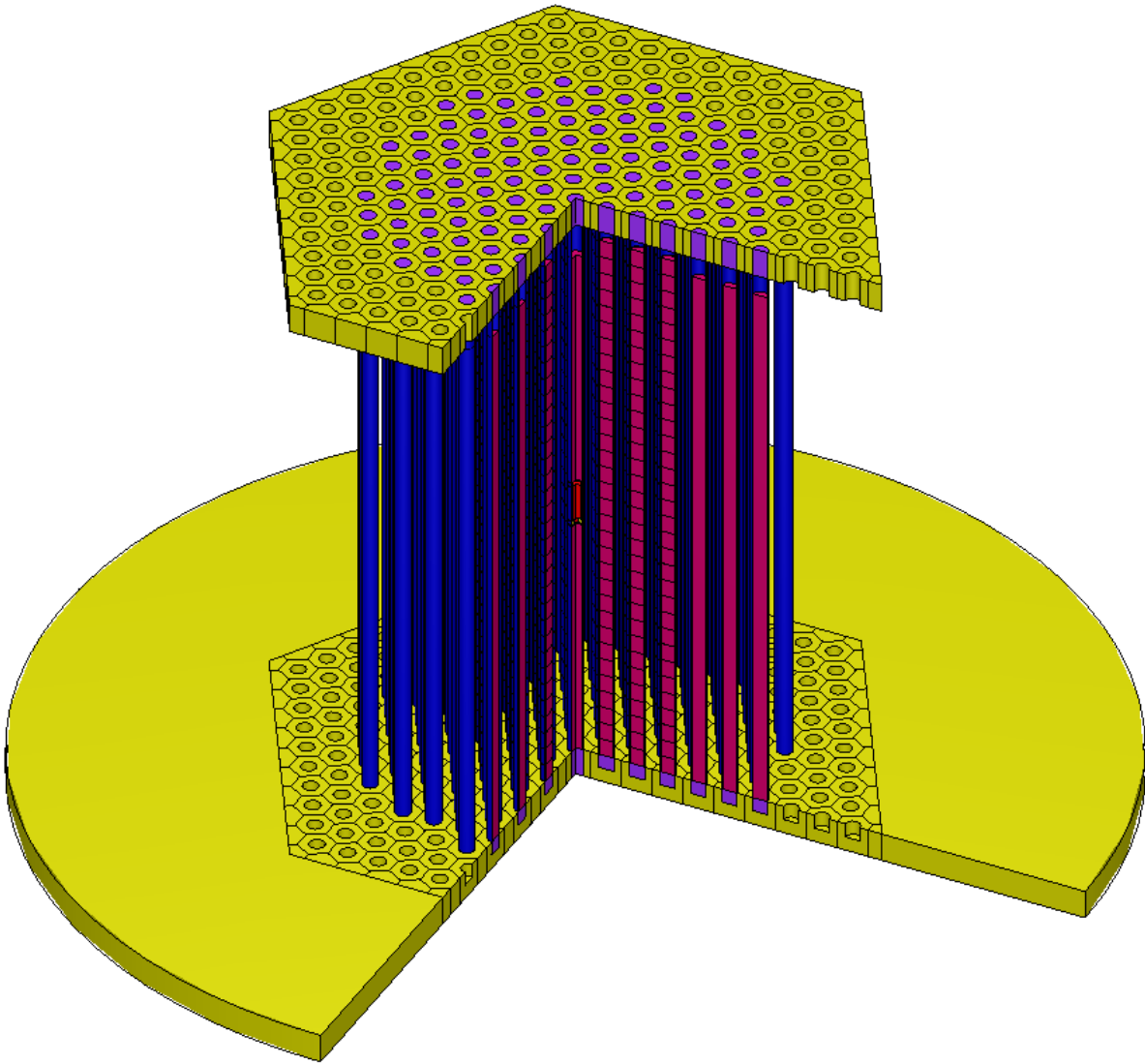


**Figure 15. LEU-COMP-THERM-079 critical configuration**

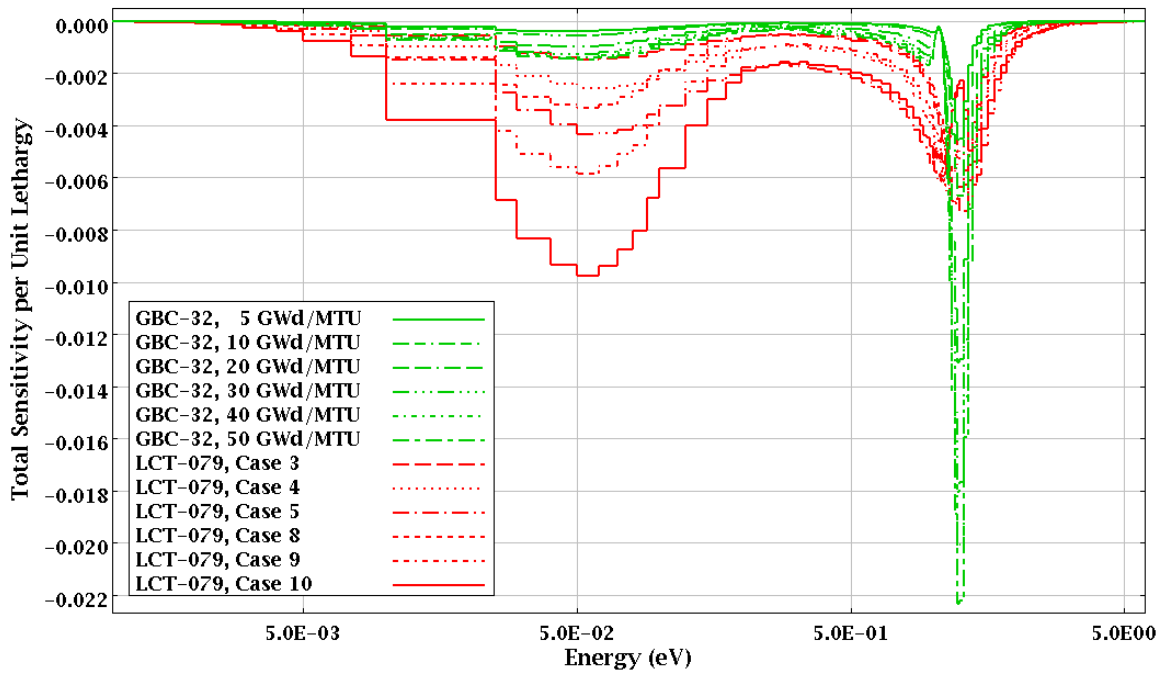
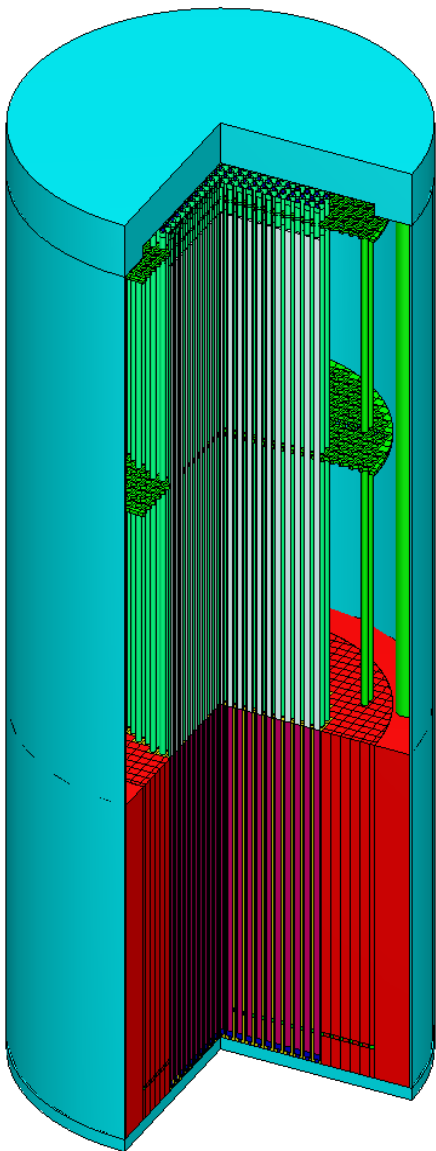


Figure 16. LEU-COMP-THERM-079 and GBC-32 <sup>103</sup>Rh sensitivity profiles

➤ **LEU-MISC-THERM-005 – FP element experiments**



**Figure 17. LEU-MISC-THERM-005 critical configurations**

This IHECSBE evaluation documents 12 critical configurations involving a square-pitch array of Zircaloy clad  $U(5.0)O_2$  fuel rods sitting in a water-reflected, cylindrical tank that is partially filled with uranyl nitrate solution ( $\sim 320$  g U/l, 6.0 wt %  $^{235}U$ ) that contains one or more of elemental Sm, Cs, Rh, and Eu. The first three cases involve three increasing concentrations of  $^{nat}Sm$ . Cases 4 through 6 involve adding concentrated  $^{nat}Cs$  solution to the Case 3 solution. Cases 7 through 9 involve adding concentrated  $^{nat}Rh$  solution to the Case 6 solution. Cases 10 through 12 were prepared by adding concentrated  $^{nat}Eu$  to the Case 9 solution. Criticality was approached by raising the level of the tank solution. Figure 17 shows a KENO3D isometric representation of one of the critical configurations.

Sensitivity profiles for  $^{149}Sm$ ,  $^{133}Cs$ ,  $^{103}Rh$ ,  $^{151}Eu$ , and  $^{153}Eu$  for the experiments and for the GBC-32 cask model are presented in Figures 18 through 22, respectively. In each of these figures, the burnup-dependent sensitivity profiles for the GBC-32 cask model are shown in green.

These experiments contain no plutonium and hence are not usable in “conventional” bias determination. Use of this data to quantify FP biases may still be possible, as is discussed later in the section on FP bias determination.

From Figure 18, the  $^{149}Sm$  profiles for the GBC-32 models and the critical configurations have similar energy dependence, with the experiments bounding the GBC-32 data. Only Cases 1 through 3 are shown. Cases 4 through 12 have  $^{149}Sm$  profiles that are similar to Case 3.

Figures 19 and 20 show the  $^{133}Cs$  and  $^{103}Rh$  profiles, respectively, for the burnup-dependent GBC-32 models and for the critical configurations. All of the curves have similar energy dependence. The experiments have adequate sensitivity to test the  $^{133}Cs$  and  $^{103}Rh$  nuclear data in the energy ranges relevant to the GBC-32 models.

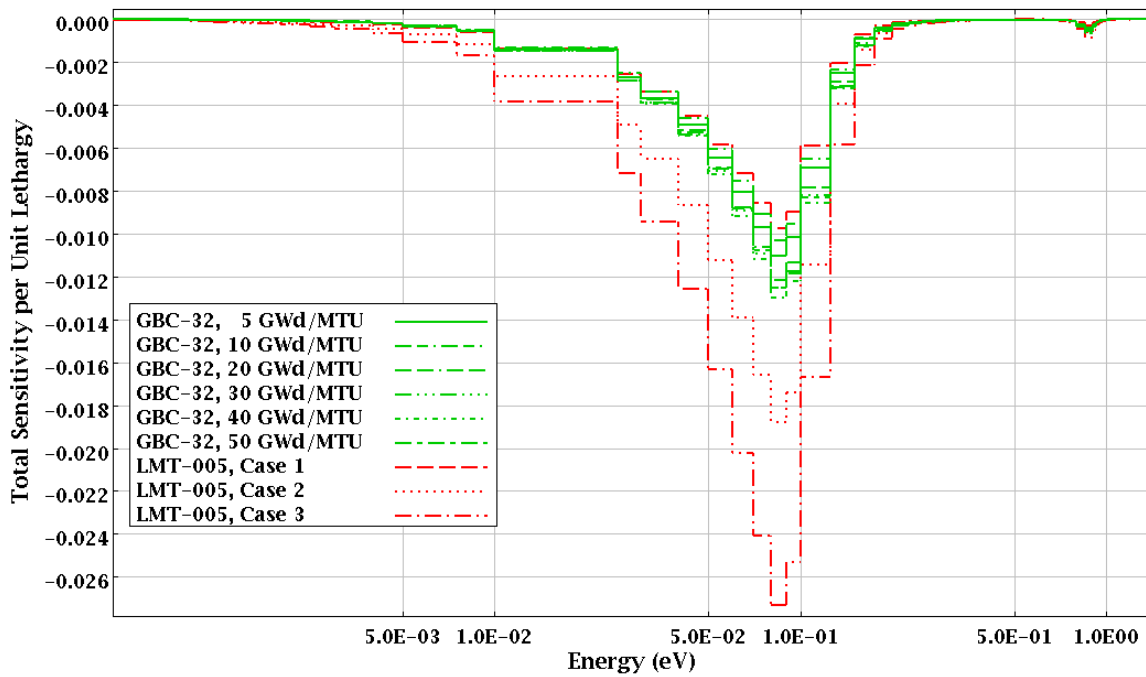


Figure 18. LEU-MISC-THERM-005 and the GBC-32  $^{149}\text{Sm}$  sensitivity profiles

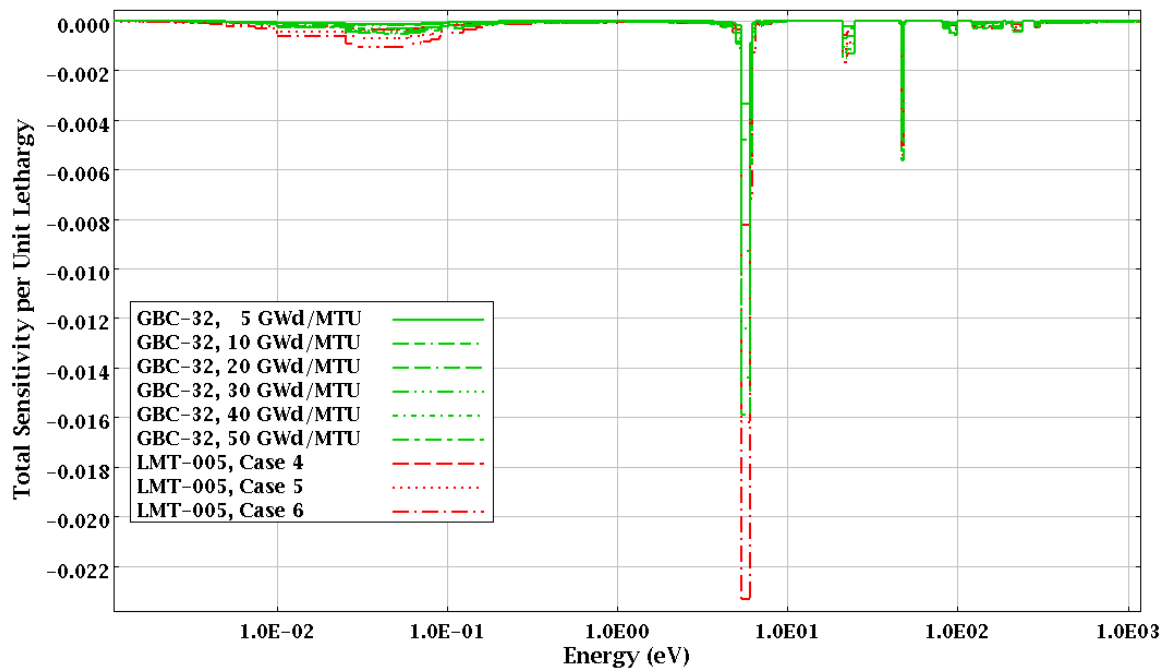
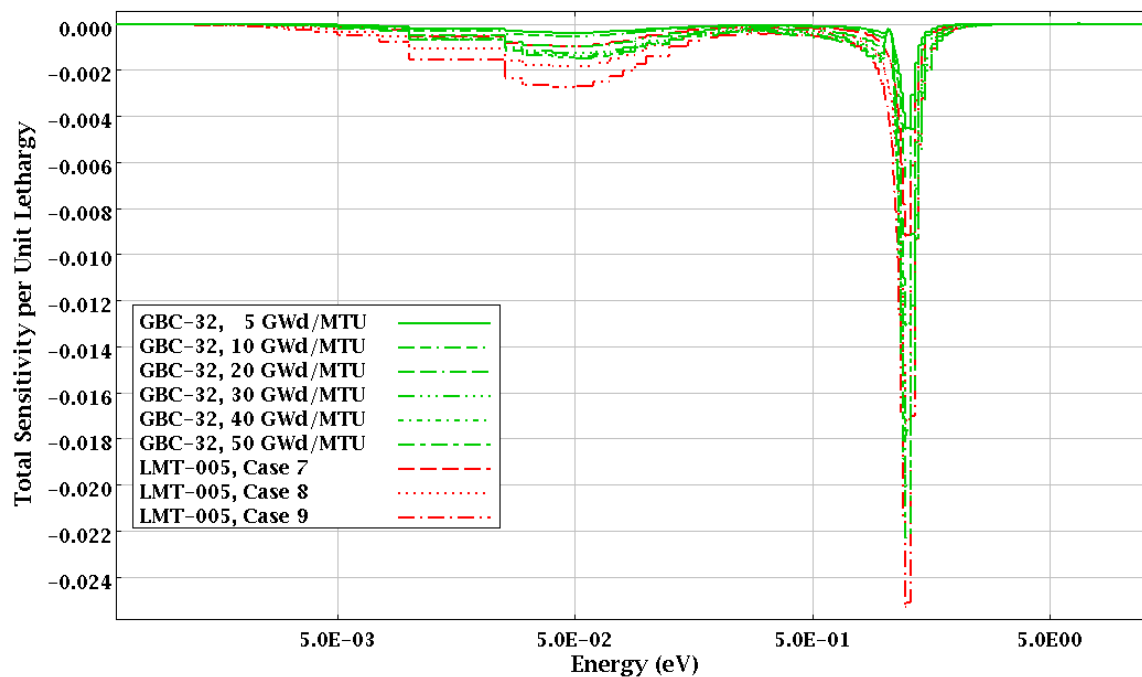
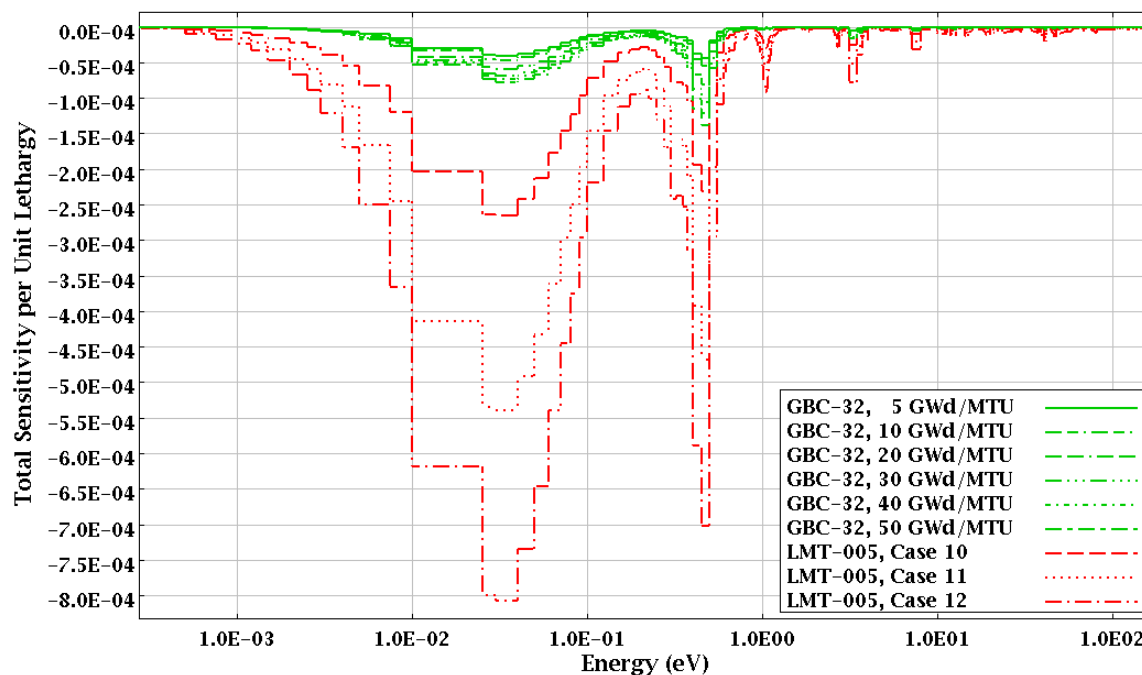


Figure 19. LEU-MISC-THERM-005 and the GBC-32  $^{133}\text{Cs}$  sensitivity profiles



**Figure 20. LEU-MISC-THERM-005 and the GBC-32  $^{103}\text{Rh}$  sensitivity profiles**

Figure 21 shows the  $^{151}\text{Eu}$  profiles for the burnup-dependent GBC-32 models and for the critical configurations. The critical configurations are considerably more sensitive to  $^{151}\text{Eu}$  than the GBC-32 models. A larger fraction GBC-32  $^{151}\text{Eu}$  sensitivity is related to the resonance at 0.5 eV. This can be seen in Figure 21 by comparing the relative heights of the peaks below 0.05 eV and at 0.5 eV. Generalized linear least-squares methods could still be used to extract  $^{151}\text{Eu}$  biases from these critical experiments.



**Figure 21. LEU-MISC-THERM-005 and the GBC-32  $^{151}\text{Eu}$  sensitivity profiles**

Figure 22 shows the  $^{153}\text{Eu}$  profiles for the burnup-dependent GBC-32 models and for the critical configurations. The critical configurations are considerably less sensitive to  $^{151}\text{Eu}$  than the GBC-32 models. The difference is so significant that the LEU-MISC-THERM-005 configurations do not provide significant validation for FP  $^{153}\text{Eu}$ .

The europium in Cases 10 through 12 is natural europium, which is 47.8 atom %  $^{151}\text{Eu}$  and 52.2 atom %  $^{153}\text{Eu}$ . The isotopic distribution of europium in burned fuel is more than 94%  $^{153}\text{Eu}$ . In the experiments, about 5% of the europium worth is from  $^{153}\text{Eu}$ , where in the GBC-32 models, about 90% of the europium worth is from  $^{153}\text{Eu}$ . Consequently, europium biases in the GBC-32 models are more likely due to  $^{153}\text{Eu}$  data, while the europium biases in the experiment models are more likely from  $^{151}\text{Eu}$  data.

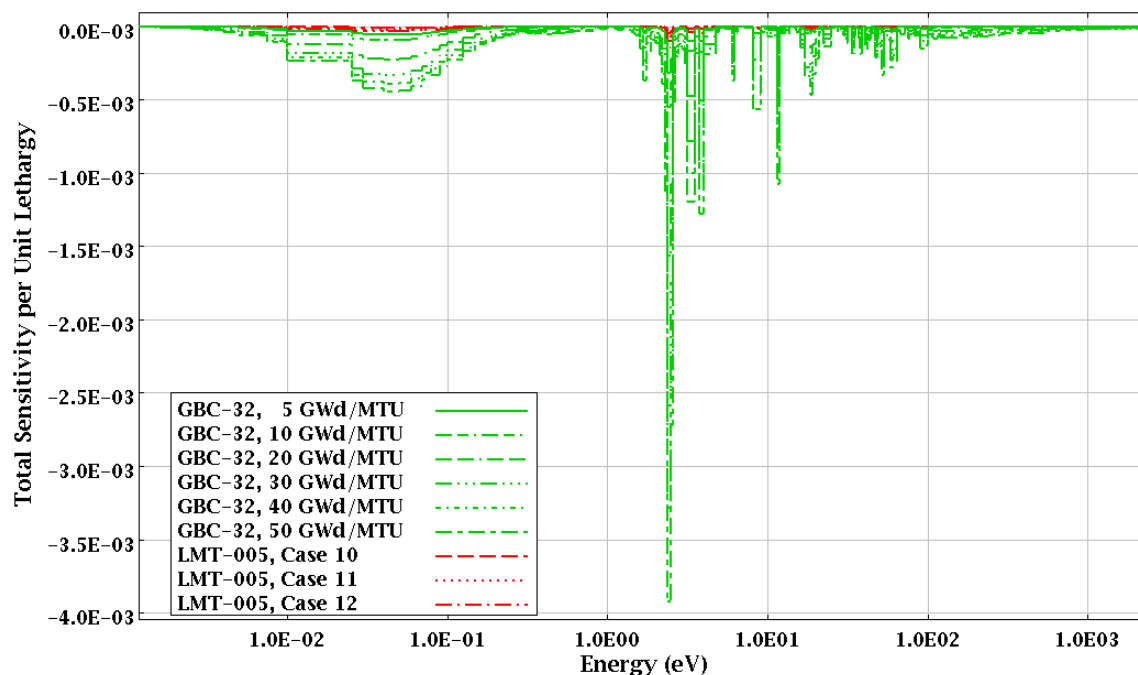


Figure 22. LEU-MISC-THERM-005 and the GBC-32  $^{153}\text{Eu}$  sensitivity profiles

➤ **HEU-COMP-INTER-005 – Case 3 –  $^{nat}\text{Mo}$  critical configuration**

A search of the 2009 edition of the IHECSBE revealed HEU-COMP-INTER-005 includes one case with molybdenum that one might try to use to validate FP  $^{95}\text{Mo}$ . Based on a neutron spectrum plot provided in the handbook, the spectrum for this critical configuration is too fast to validate  $^{95}\text{Mo}$  in a typically flooded, well-moderated burnup credit SA model.

➤ **IHECSBE experiments with natural gadolinium**

Approximately 210 critical configurations involving  $^{155}\text{Gd}$  are documented in the 2009 IHECSBE. Unfortunately, the  $^{155}\text{Gd}$  is present in natural gadolinium. Burned nuclear fuel contains no  $^{157}\text{Gd}$  because it is consumed in the reactor as it is created, and the  $^{157}\text{Gd}$  radioactive decay precursors have relatively short half-lives, resulting in little build-up after power generation. The  $^{155}\text{Gd}$  is also consumed during operation, but its regeneration continues after shutdown due to the decay of  $^{155}\text{Eu}$ , with a 4.75-year half-life, to  $^{155}\text{Gd}$ . As a result of these processes,  $^{155}\text{Gd}$  is present in burned fuel for which a minimum cooling time of 5 years is typically required and  $^{157}\text{Gd}$  is not present at significant levels.

Natural gadolinium contains 14.8 atom %  $^{155}\text{Gd}$ , which has a thermal neutron  $n,\gamma$  reaction cross section of 61,000 barns, and 15.65 atom %  $^{157}\text{Gd}$ , which as a thermal neutron  $n,\gamma$  reaction cross section of 255,000 barns. While critical experiments with  $^{nat}\text{Gd}$  can be used to quantify a bias present due to the  $^{nat}\text{Gd}$ , it is not possible to use these experiments to quantify how much of that bias is due to  $^{155}\text{Gd}$ . Since the publicly available critical experiments do not contain gadolinium significantly enriched in  $^{155}\text{Gd}$ , they cannot be used to quantify a bias associated with FP  $^{155}\text{Gd}$ .

➤ **REBUS Program – spent fuel configurations**

As part of the REBUS Program, two critical configurations that included some burned fuel were assembled [22, 23]. Figure 23 shows a KENO3D image of the REBUS configuration containing burned  $\text{UO}_2$  fuel. The central  $7 \times 7$  spent fuel bundle segment included a  $5 \times 5$  array of burned fuel rods. The spent fuel bundle was placed in the middle of a  $27 \times 27$  array of fresh  $\text{UO}_2$  fuel rods. The array was water moderated and reflected. Criticality was approached by raising the water level. Figure 24 shows the  $^{239}\text{Pu}$  fission sensitivity profiles for one of the GBC-32 models and for the REBUS spent fuel critical configuration. Note that the GBC-32 model is 15 times more sensitive to the  $^{239}\text{Pu}$  cross sections than the REBUS configuration. The overall bias calculated for the REBUS spent fuel configuration would be much closer to the bias calculated for a fresh low-enrichment uranium system. Additionally, Figures 25 through 27 show the sensitivity profiles for the GBC-32 model with fuel burned to 40 GWd/MTU and the REBUS spent fuel configuration for FPs  $^{149}\text{Sm}$ ,  $^{143}\text{Nd}$ , and  $^{103}\text{Rh}$ , respectively. The sensitivity for these three FPs is far lower than the sensitivities exhibited by the GBC-32 model. Hence, these critical configurations are not suitable for a conventional bias determination analysis for spent fuel.

The REBUS program data is not publicly available.

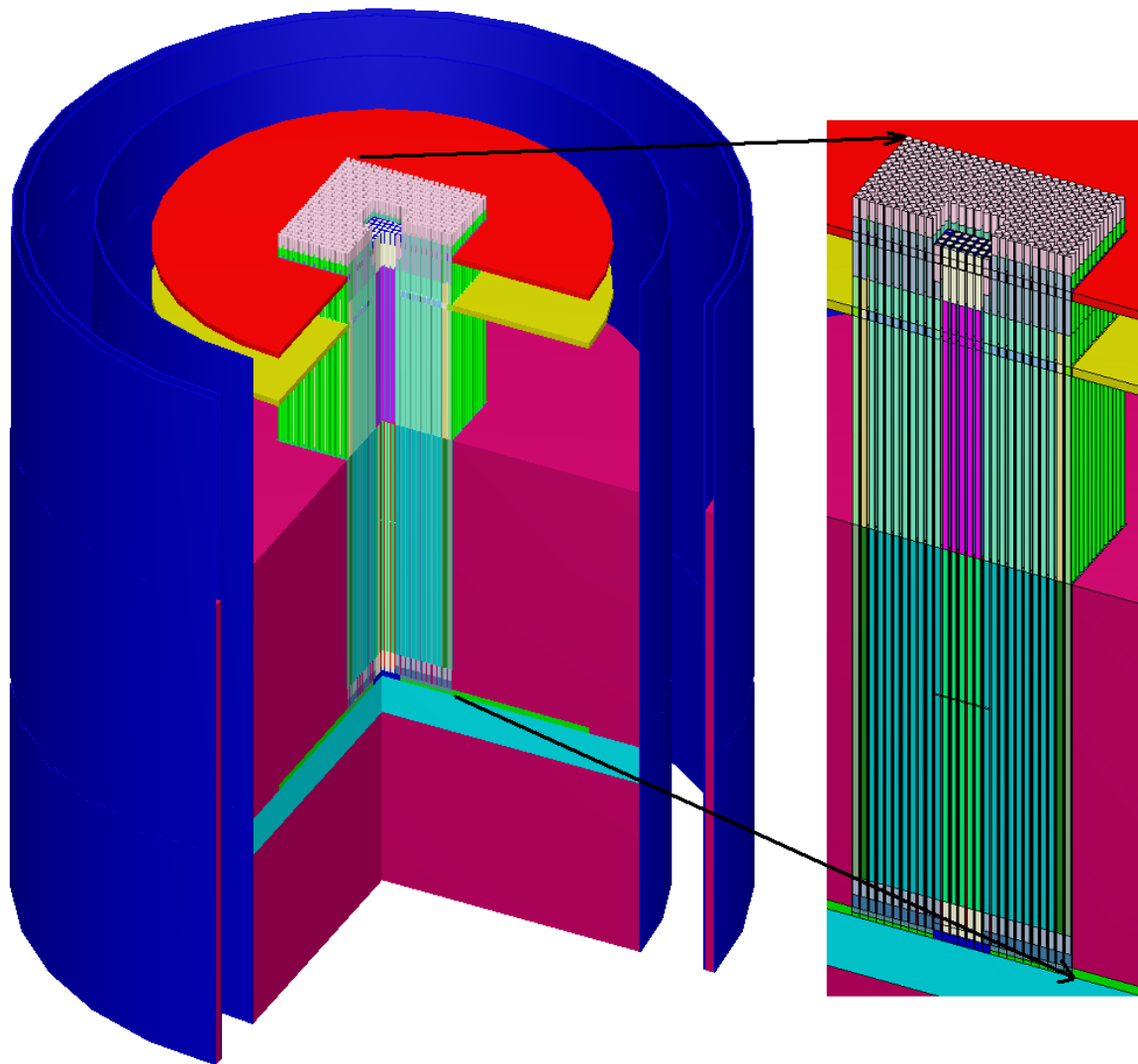


**Figure 23. REBUS spent fuel configuration**

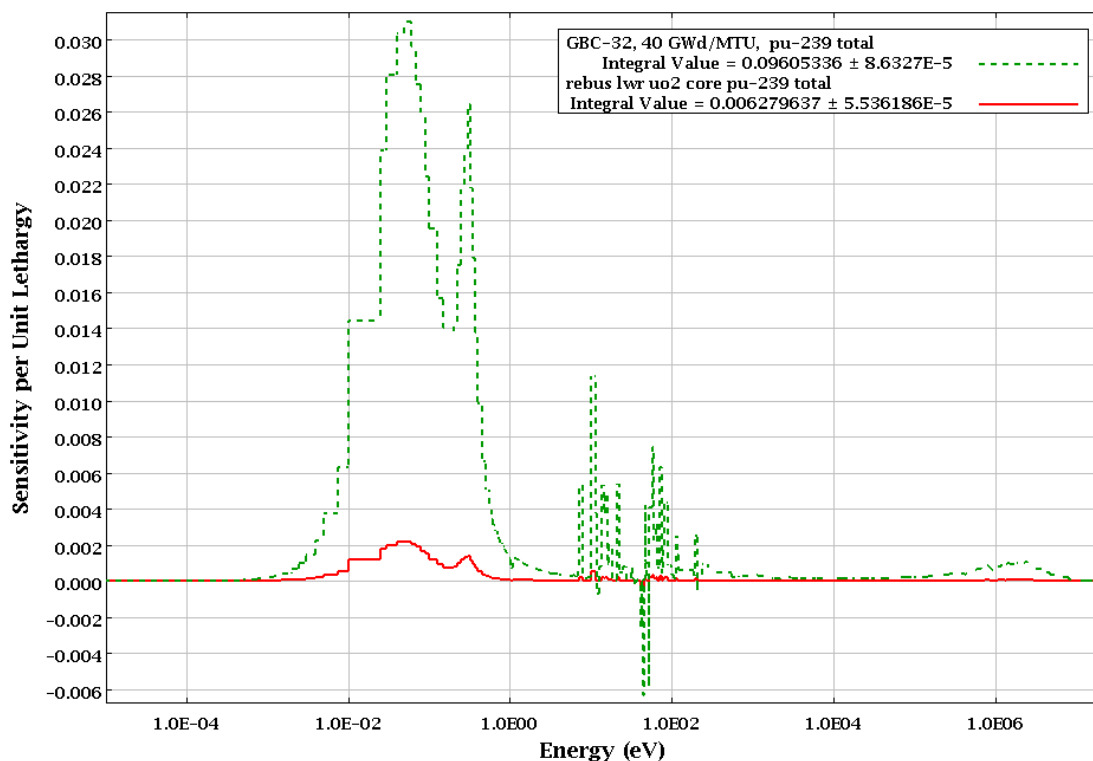


Figure 24. GBC-32 and REBUS spent fuel configuration  $^{239}\text{Pu}$  total sensitivity profiles

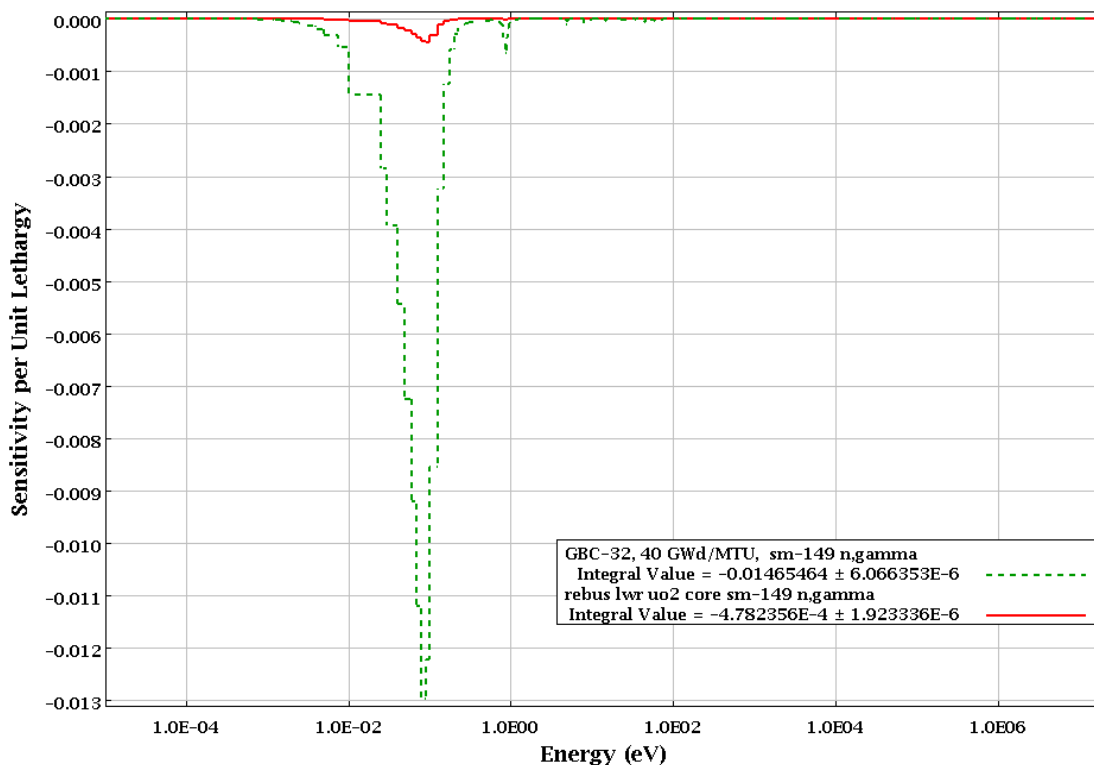


Figure 25. REBUS spent fuel configuration and GBC-32  $^{149}\text{Sm}$  n, $\gamma$  sensitivity profiles

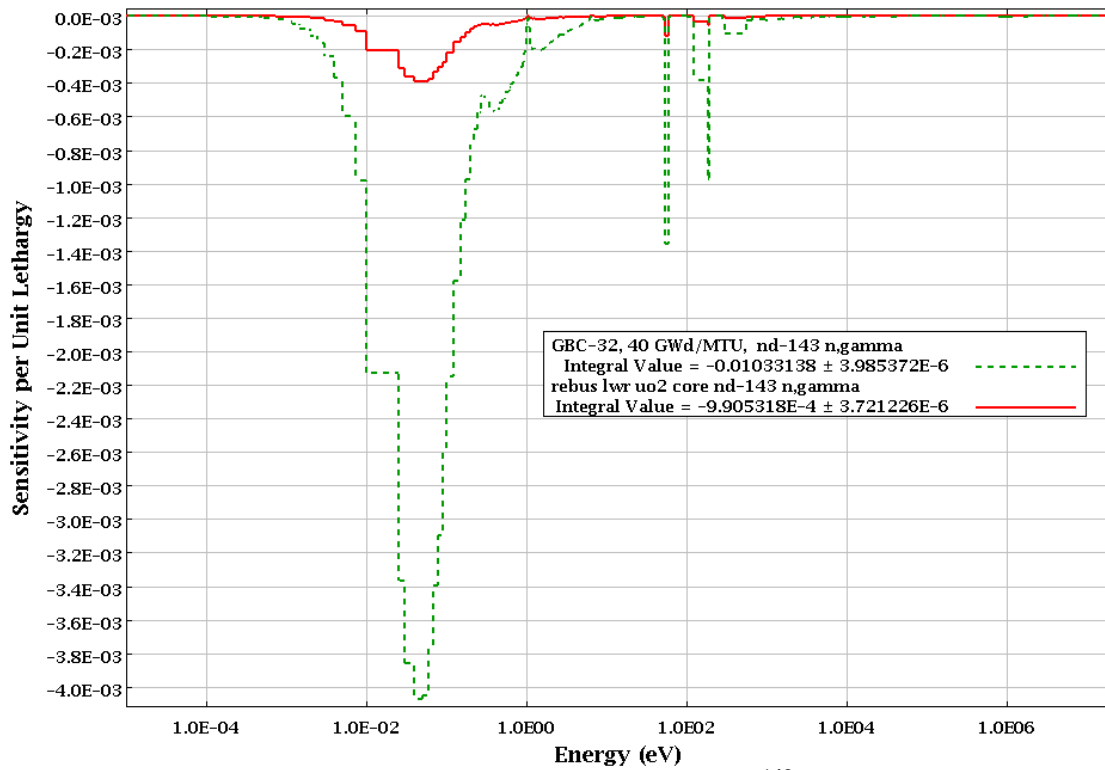


Figure 26. REBUS spent fuel configuration and GBC-32  $^{143}\text{Nd}$  n,γ sensitivity profiles

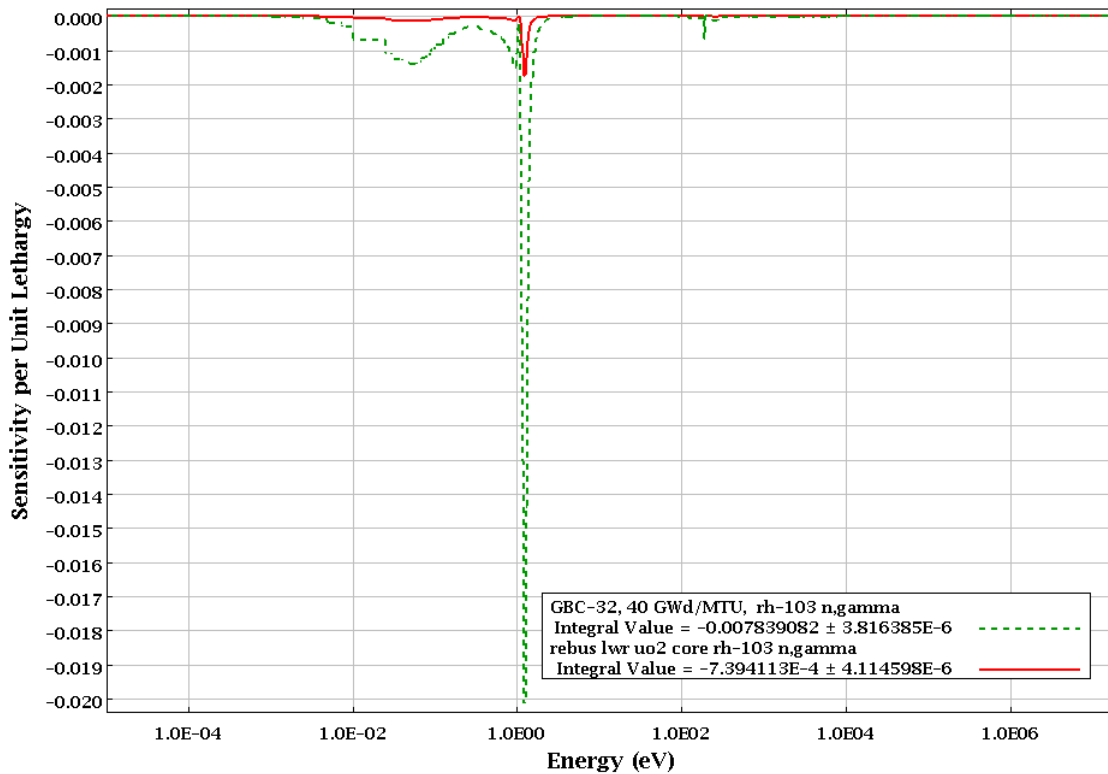


Figure 27. REBUS spent fuel configuration and GBC-32  $^{103}\text{Rh}$  n,γ sensitivity profiles

➤ **MINERVE FP reactivity worth measurements**

Experiments have been conducted with the French Minerve [24] and British Dimple [25] reactors in which the reactivity worth of FP samples was measured by oscillating the sample in and out of the reactor and calculating the sample worth from its measured impact on reactor period. These sample worth measurements have been compared to calculated values to quantify potential biases in  $k_{eff}$  calculations involving FPs [25, 26, 27].

To date, the detailed descriptions of these experiments have not been publicly available. Consequently, we have not been able to assess the usefulness of these measurements for calculating FP biases.

FP bias and bias uncertainty for the reactor geometries may be inferred by comparing calculated and measured FP worths. Due to potential differences in neutron spectra, 3-D effects, and low FP worth, it is not clear that such biases and bias uncertainties would be applicable to burned fuel storage, transportation, and disposal systems. Reactivity sensitivity and uncertainty analysis techniques developed at ORNL may be well suited for utilizing reactivity worth measurements to estimate FP bias and bias uncertainty. More information on the use of SCALE TSAR and TSURFER programs is presented later in this paper.

➤ **French FP experiments**

A series of 145 critical configurations[20], including 73 configurations with one or more of FP nuclides  $^{103}\text{Rh}$ ,  $^{133}\text{Cs}$ ,  $^{\text{nat}}\text{Nd}$ ,  $^{149}\text{Sm}$ ,  $^{152}\text{Sm}$ , and  $^{155}\text{Gd}$ , was performed by CEA at the Valduc Facility near Dijon, France. The fission material involved was a combination of  $\text{U}(4.7)\text{O}_2$  rods and HTC ( $\text{PuO}_2$  and  $\text{UO}_2$ ) rods. Some of the experiments were similar to the LEU-COMP-THERM-050 experiments discussed earlier in this paper.

These data are not publicly available. It is likely that these data could be used in a data adjustment technique to estimate bias and bias uncertainties for the FPs utilized in the experiments.

➤ **Commercial Reactor Criticals (CRCs)**

Ideally, well-characterized critical experiments involving spent fuel should be used for validation of spent fuel criticality calculations. Thus there has been some interest in trying to use operating data from commercial nuclear power plants to validate BUC calculations.

Detailed data describing near-critical configurations of several commercial nuclear power plants have been collected and used to generate models that could be useful for validation of  $k_{eff}$  calculations for systems with burned nuclear fuel assemblies [28]. The information includes reactor geometry and reactor parametric (e.g., temperatures, power levels, water densities, soluble boron concentrations, etc.) information that is from one or more operating cycles and is used to calculate the fuel compositions used in a CRC statepoint model. The  $k_{eff}$  value calculated

for a CRC statepoint may then be compared to the  $k_{eff}$  value expected for the model to quantify the bias for the CRC statepoint models. Because the CRC statepoint data sets describe real systems with real actinide and FP compositions, the statepoints involving burned fuel should be useful for validating  $k_{eff}$  calculations for burned fuel storage and transportation systems. The bias and bias uncertainty calculated using the CRC models includes bias and bias uncertainty associated with both calculation of burned fuel compositions and calculation of  $k_{eff}$  for the CRC models. Figure 28 (extracted from Ref. 28) shows typical overhead and side views of a CRC model. Note from the figure that even simplified CRC models are rather complex.

Figures 29 through 34 show comparisons of sensitivity profiles from the GBC-32 models and models from Crystal River Unit 3 statepoints 2, 19, and 33, which have core average burnup values of 8, 20, and 33 GWd/MTU, respectively. The figures show that the GBC-32 models are qualitatively similar to the Crystal River statepoint models.

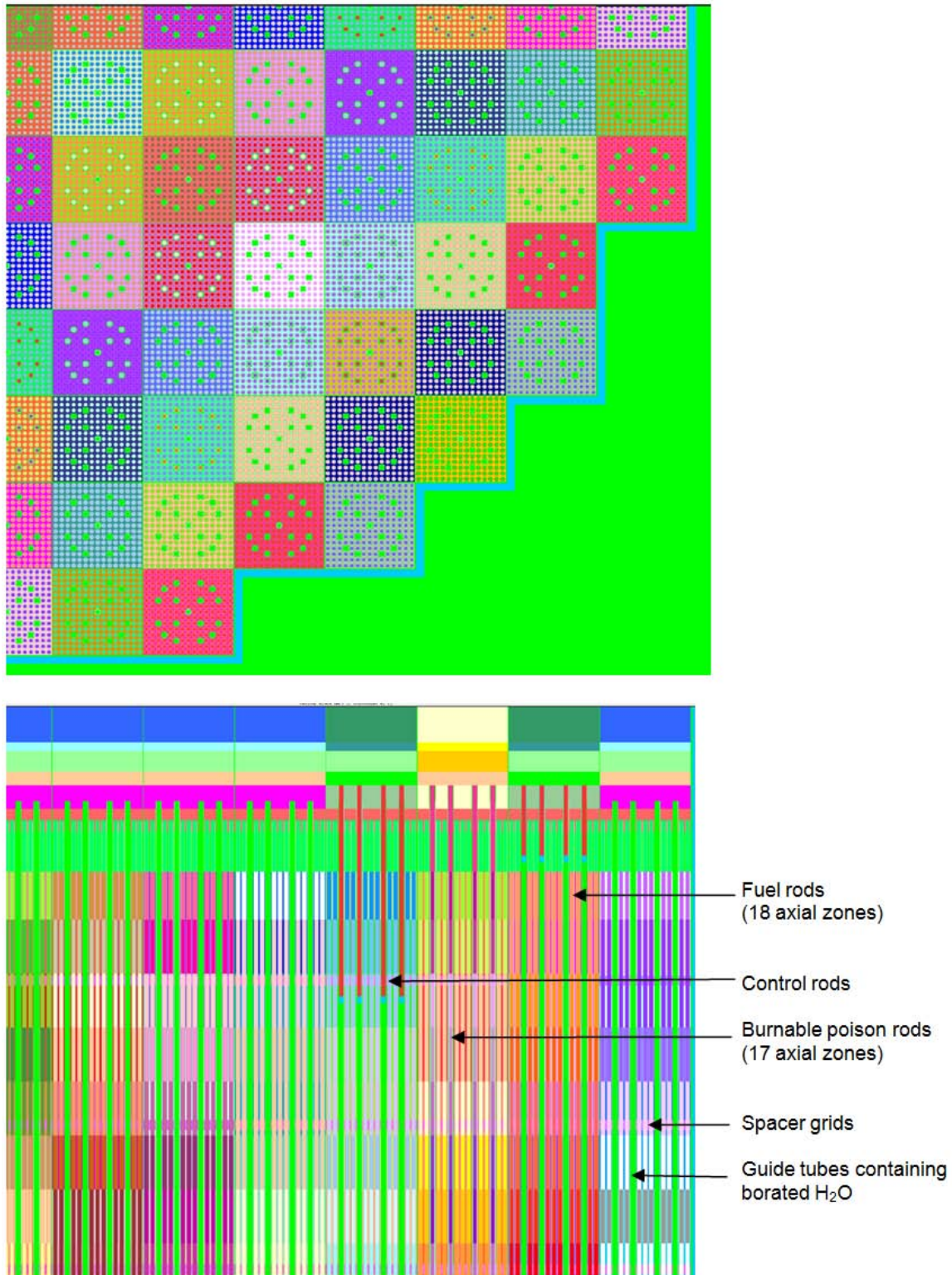


Figure 28. Top and side views of a CRC model (figure extracted from Ref. 28)

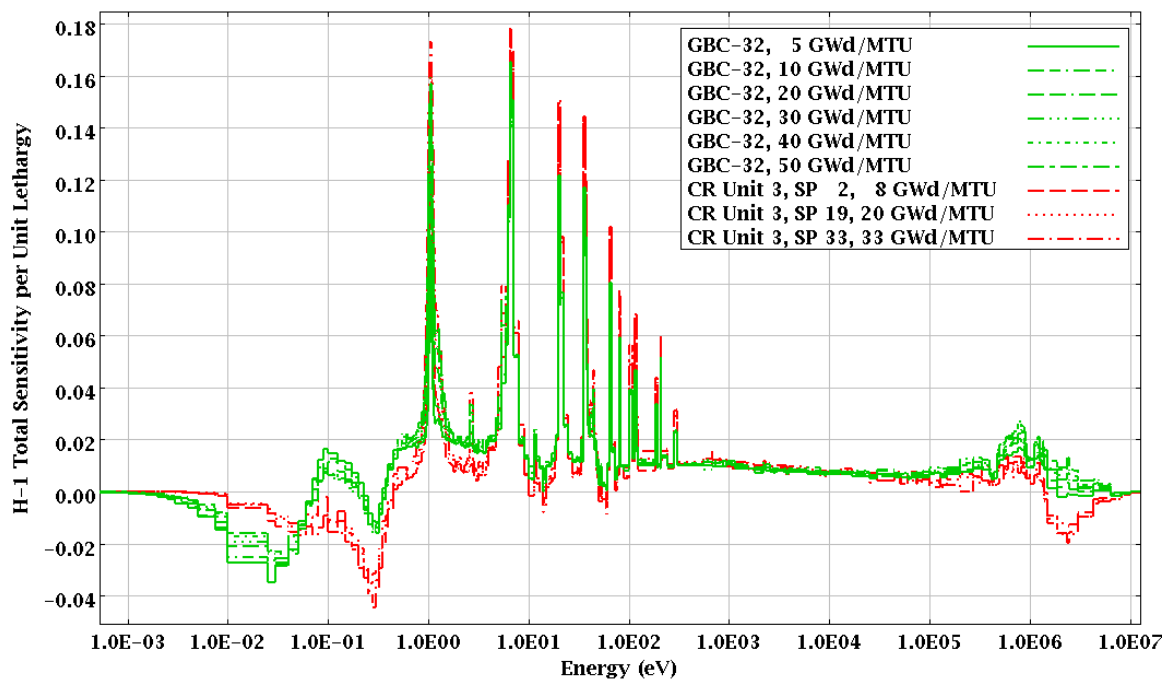


Figure 29. Comparison of GBC-32 and CRC  $^1\text{H}$  total sensitivities

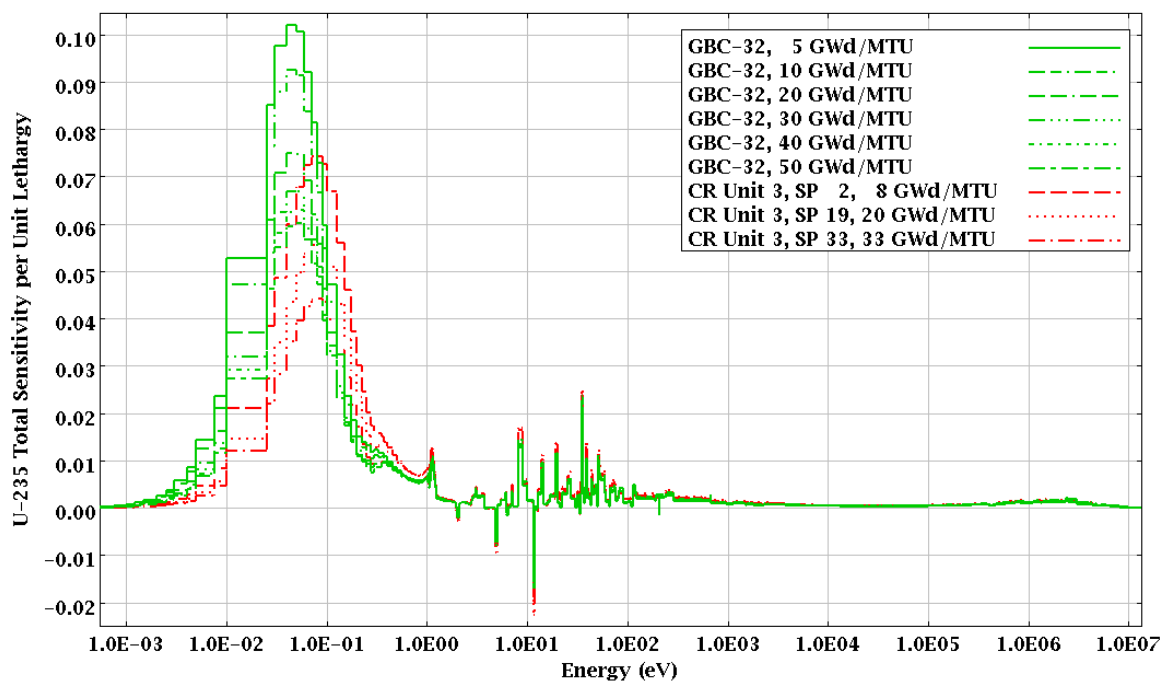


Figure 30. Comparison of GBC-32 and CRC  $^{235}\text{U}$  total sensitivities

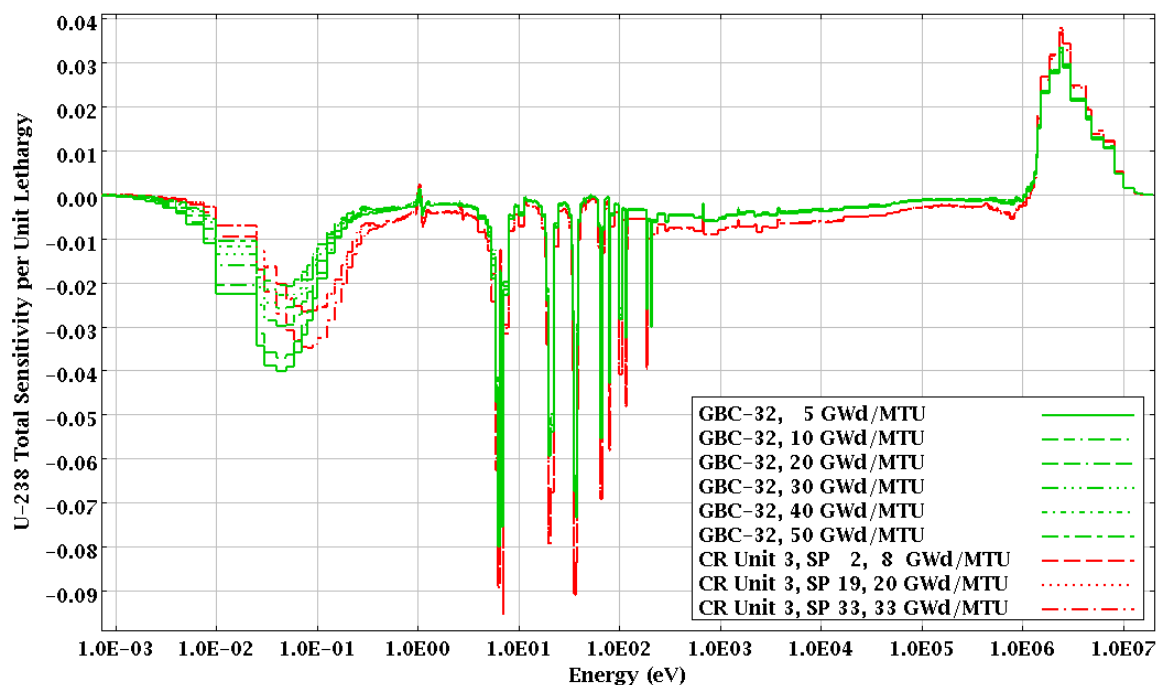


Figure 31. Comparison of GBC-32 and CRC  $^{238}\text{U}$  total sensitivities

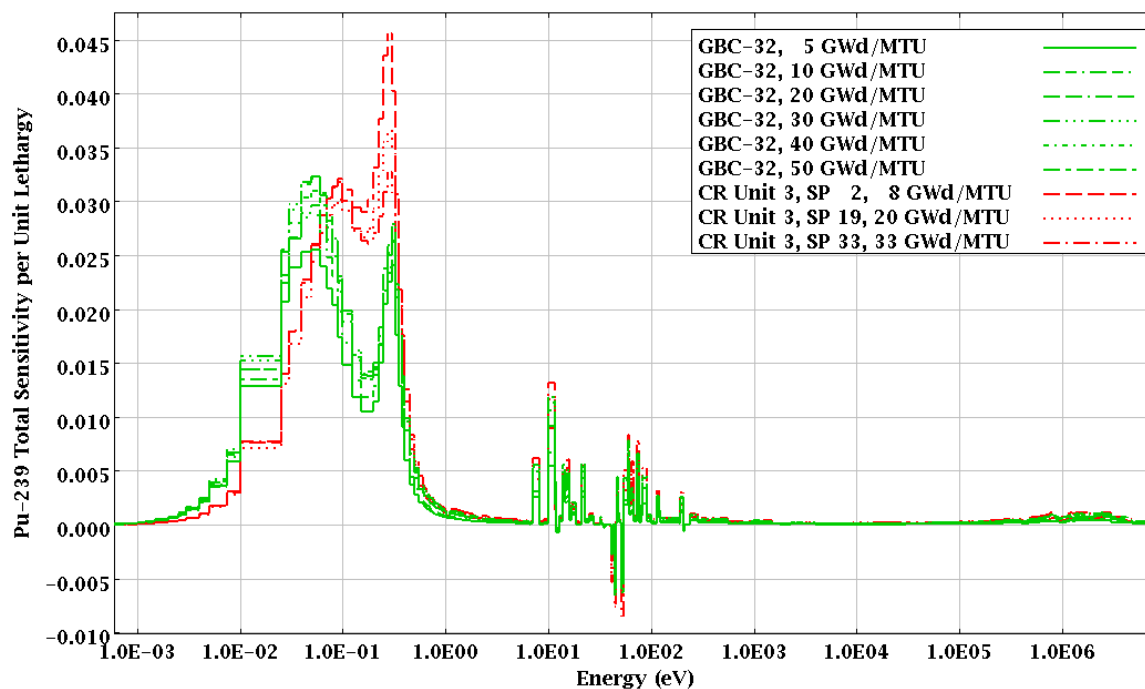


Figure 32. Comparison of GBC-32 and CRC  $^{239}\text{Pu}$  total sensitivities

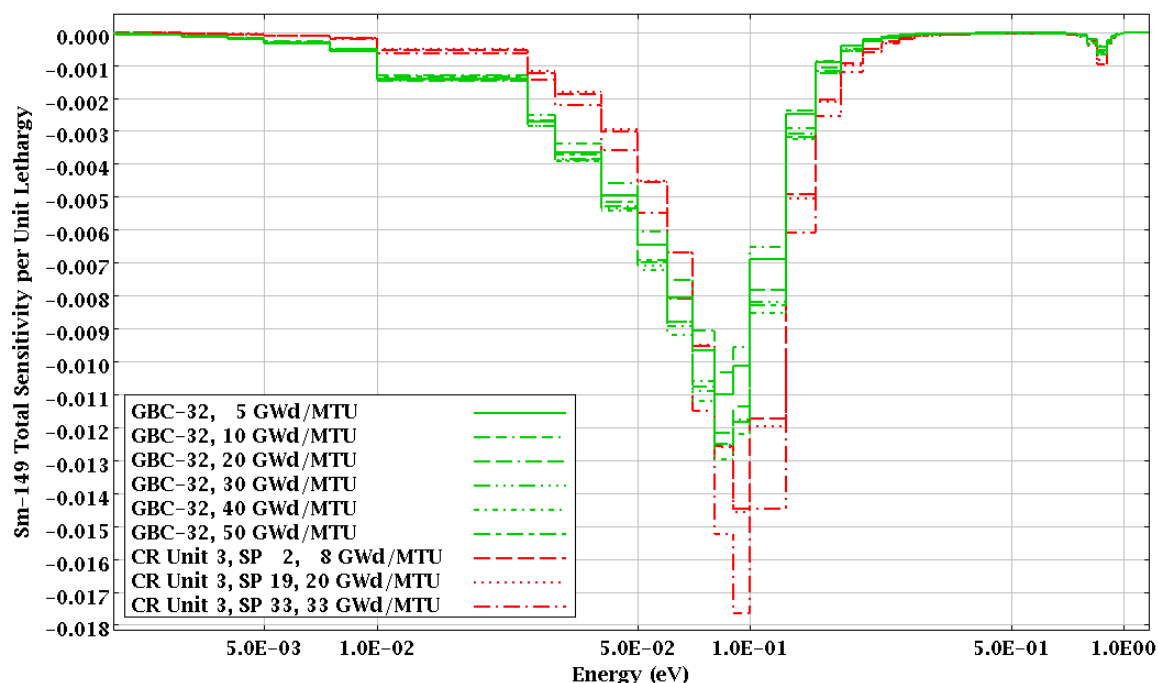


Figure 33. Comparison of GBC-32 and CRC  $^{149}\text{Sm}$  total sensitivities

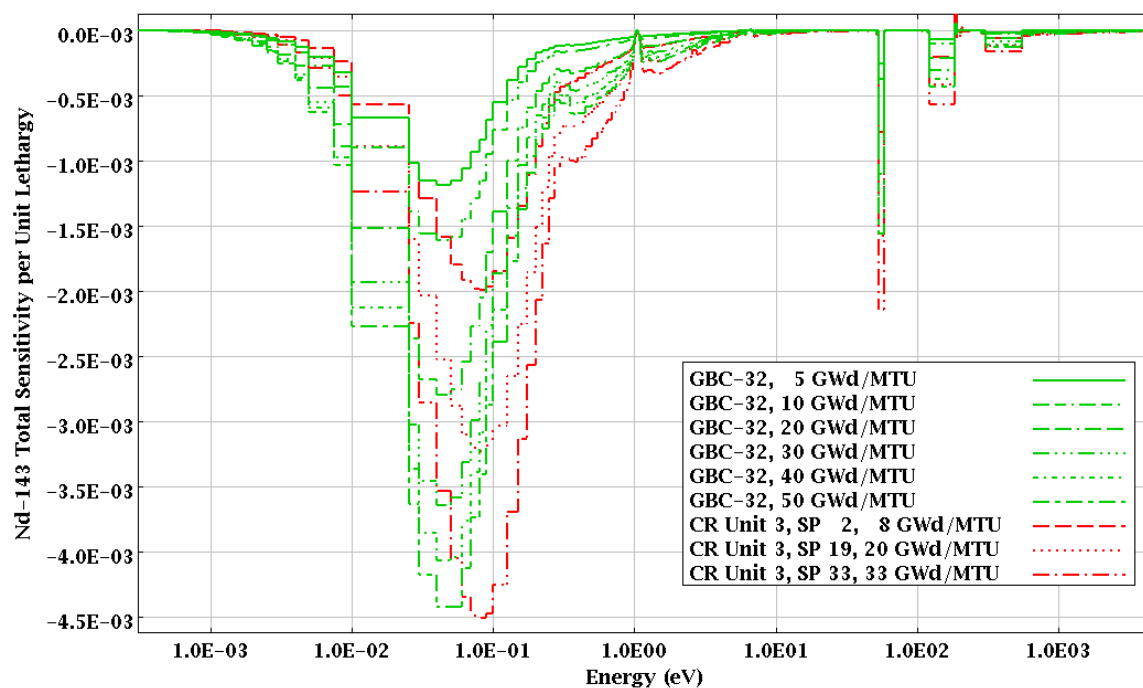


Figure 34. Comparison of GBC-32 and CRC  $^{143}\text{Nd}$  total sensitivities

Some have questioned the suitability of CRCs for validation because the reactivity of the operating plants is driven primarily by low-burnup fuel, and the bias associated with the low burnup fuel could be different from the bias associated with the higher burnup values typically credited in BUC analyses. In response to this concern, ORNL evaluated the similarity of the

CRC models to burned fuel systems. The ORNL evaluation [28] used sensitivity and uncertainty analysis techniques to show that for most cases the CRC models were adequately similar to burned fuel systems with burnups between 10 and 60 GWd/MTU. The similarity determination was based on the SCALE  $c_k$  parameter, which is a correlation coefficient indicating the amount of shared uncertainty in  $k_{eff}$  between two systems.

There are a few issues associated with the use of the CRCs for validation that need to be addressed. First is that the CRC models are large and complicated, requiring significant computing resources. Second, significant approximations and assumptions need to be made to create the CRC models. Typically, the expected or measured  $k_{eff}$  values for laboratory critical experiments should be adjusted to account for the impact of approximations. The biases and uncertainties associated with the CRC modeling approximations and assumptions have not been quantified. A third issue is that the CRCs are all at significantly elevated temperatures. As is reported in Ref. 28, the fuel temperatures for the evaluated CRCs ranged from 550 to 910 K. Safety analyses for spent fuel are generally performed at temperatures between 273 and 373 K. The bias and bias uncertainty adjustment associated with the CRC elevated temperatures have not been quantified. A fourth issue is that the CRCs contain other materials that are typically not present in the SA models, such as control rods, additional FPs, removable burnable absorber rods, etc. It is not clear how to adjust a bias calculated using the CRCs to account for bias and bias uncertainty associated with the extra materials that are not present in the SA models. These issues should be addressed if the CRCs are used to validate BUC calculation methods.

## **FP BIAS ESTIMATION**

The correct bias and bias uncertainty for a safety analysis model is determined using critical experiments that respond to the same nuclear data in the same way. That is to say that the critical experiments should have the same materials and same energy-dependent  $k_{eff}$  sensitivity to nuclear data variation as the SA model. Any materials present in the experiments and not present in the SA model or present in the SA model and not present in the critical configurations produce some error in the calculated bias and should increase the bias uncertainty. Variations in the neutron energy spectra between SA models and critical configurations also produce some error in the calculated bias and should increase bias uncertainty.

There are no very well-characterized (e.g., laboratory experiment) critical configurations containing uranium, plutonium, and FPs, all in the right proportions, to support calculation of a single bias appropriate for FP BUC SA models. An alternative is to address the potential gaps in the FP BUC validation data by estimating FP biases separately.

Bounding estimates for FP biases could be based on the uncertainties in  $k_{eff}$  due to uncertainties in FP nuclear data, as presented in Table 1 and Figure 10.

There are a few techniques that may be useful to determine FP-specific biases. One might use a carefully crafted series of critical experiments in which some of the critical configurations have the FP and some do not. Then bias and bias uncertainty could be calculated for each subset. The difference between the bias and bias uncertainties for the two subsets should be the bias and bias

uncertainty for the targeted FP. The design of the FP configurations must include some positive reactivity change to offset the addition of the FP. Consequently, the difference between with FP and without FP biases will also include bias and bias uncertainty associated with the mechanism used to add reactivity. Finally, care must be taken in determining how the FP bias should be applied to the SA model. To be statistically significant, the FP will likely be present in the critical configuration at a larger reactivity worth than it is in the SA model. The bias and bias uncertainty would need to be adjusted to be applicable to the SA model. Further, for the FP bias and bias uncertainty from the critical configurations to be applicable to SA model, it is necessary that the critical configurations and SA model have similar FP sensitivity energy-dependence. Some work has been performed by Roberts [29] to quantify the uncertainty related to variation in sensitivity profile energy dependence.

### **Generalized Linear Least-Squares Method (TSURFER)**

Another technique under development at ORNL is the generalized linear least-squares method, sometimes called nuclear data adjustment, implemented in the SCALE Tool for Sensitivity and Uncertainty Analysis of Response Function using Experimental Results (TSURFER) program. This method uses (1) sensitivity data calculated for a set of critical experiments and for the SA model using the SCALE TSUNAMI-1D/3D sequences, (2) the cross-section covariance data distributed with SCALE 6, and (3) user input values for the critical experiment expected  $k_{eff}$  values and uncertainties, including uncertainty correlations between critical configurations. TSURFER combines the sensitivity and uncertainty data to identify the set of nuclear data and experimental  $k_{eff}$  value adjustments that will minimize the overall chi-squared statistic for the adjustments. The process includes some techniques for rejecting data for which the adjustments appear to be inconsistent with the uncertainties in the values. TSURFER uses the set of adjustments and a modified uncertainty matrix to estimate the impact of the adjustments on the SA model and to quantify the residual uncertainty in  $k_{eff}$  due to nuclear data uncertainties following the data adjustment. The difference between pre-adjustment and post-adjustment SA model  $k_{eff}$  values is the bias. The bias uncertainty is assumed to be bounded by the residual post-adjustment uncertainty in  $k_{eff}$  due to nuclear data uncertainties.

Note that TSURFER does not produce modified cross-section libraries. Instead, it uses the sensitivity data to infer how the system  $k_{eff}$  is affected by data perturbation. It is interesting that nuclear data evaluators are showing strong interest in using tools like TSURFER to help them identify nuclear data that perhaps needs to be revised.

TSURFER requires sensitivity data from critical configurations with FPs in order to calculate bias and bias uncertainty values associated with FPs. Unfortunately, there are few publicly available well-characterized critical configurations with FPs. For demonstration purposes, a TSURFER calculation was performed using the sensitivity data from the 18 cases of LEU-COMP-THERM-050, the 10 cases from LEU-COMP-THERM-079, the 12 cases from LEU-MISC-THERM-005, and 189 other low-enrichment uranium, intermediate-enrichment uranium, high-enrichment uranium, plutonium, and mixed uranium and plutonium systems. The bias results from this calculation for the GBC-32 cask model loaded with fuel burned to 50

GWd/MTU are presented in Table 2 along with the uncertainties in  $k_{eff}$  due to nuclear data uncertainties that were presented earlier in this paper.

**Table 2. TSURFER FP Bias Calculation Results for GBC-32 Loaded with Westinghouse 17 × 17 Assemblies with 50 GWd/MTU Burnup**

	Nuclear Data Uncertainty <sup>†</sup>		TSURFER	
	(dk/k)	(pcm)	bias (pcm)	uncert (pcm)
<sup>95</sup> Mo	6.10E-05	5.75	0.61	5.72
<sup>99</sup> Tc	8.43E-05	7.95	n.e.*	7.95
<sup>101</sup> Ru	9.62E-05	9.07	n.e.	9.07
<sup>103</sup> Rh	2.37E-04	22.38	-6.79	15.47
<sup>109</sup> Ag	2.79E-05	2.63	n.e.	2.63
<sup>133</sup> Cs	1.94E-04	18.32	12.00	14.43
<sup>143</sup> Nd	3.88E-04	36.62	n.e.	36.62
<sup>145</sup> Nd	2.00E-04	18.88	n.e.	18.88
<sup>147</sup> Sm	6.41E-05	6.04	0.08	6.04
<sup>149</sup> Sm	2.08E-04	19.60	4.46	12.30
<sup>150</sup> Sm	6.69E-05	6.31	0.05	6.10
<sup>151</sup> Sm	1.36E-04	12.86	n.e.	12.86
<sup>152</sup> Sm	6.98E-05	6.58	0.43	6.57
<sup>151</sup> Eu	2.68E-06	0.25	-0.03	0.25
<sup>153</sup> Eu	9.00E-05	8.49	-0.12	8.49
<sup>155</sup> Gd	5.15E-05	4.86	0.37	4.86
Combined	6.26E-04	59.03	11.07	53.47

<sup>†</sup> From Table 1

\* n.e. means "no experiments"

The columns under "Nuclear Data Uncertainty" show the uncertainty in  $k_{eff}$  due to the original uncertainty in the nuclear data from Table 1 and are provided for comparison with the TSURFER results. Due to the small amount of sensitivity data available for critical systems with FPs, the bias estimates have uncertainties that are larger than the calculated biases. A positive bias value means the unadjusted FP cross sections are too low, causing the calculated  $k_{eff}$  value to be too high.

Due to the small reduction in uncertainty, there is little value in drawing conclusions based solely on the TSURFER results presented in Table 2. Use of additional critical experiment data with FPs may significantly reduce the bias uncertainty and thus provide more useful bias and bias uncertainty estimates.

## Reactivity Sensitivity Analysis (TSAR)

A reactivity sensitivity analysis method has been implemented in the SCALE TSAR (Tool for Sensitivity Analysis of Reactivity) program that computes reactivity sensitivities [30] from  $k_{eff}$  sensitivity data computed using TSUNAMI-1D or -3D. TSAR also computes reactivity uncertainty using the reactivity sensitivity data and cross-section covariance data.

TSAR subtracts sensitivity data associated with one state from the sensitivity data from a second state, producing a sensitivity data file that shows how nuclear data perturbations can affect the change in neutron multiplication between the two states. Consider for example the reactivity oscillation experiments described earlier in this paper. The initial state could be considered to be the experiment with no FP sample present. The second state would then be similar to the first experiment, but would include a FP sample. The change in the reactor period would be measured and the reactivity worth for the change from state one to state two inferred from the change in reactor period. TSUNAMI-1D, -2D, or -3D is used to calculate  $k_{eff}$  sensitivity data for both of the states. TSAR is then applied to calculate the sensitivity of the reactivity difference between the two states to variations in nuclear data. If the calculated and measured reactivity values differ, TSURFER could be applied to identify nuclear data adjustments that would make the measured and calculated reactivity worth values agree. TSURFER would also use the  $k_{eff}$  sensitivity data for a SA model with the adjustments to the FP cross sections to quantify the bias and bias uncertainty associated with the test material that is applicable to the SA model.

The TSAR technique focuses on the changes between two variations of a system. Thus sensitivities and biases that are common to both states are ignored. This magnifies the importance of the material or feature targeted by the variation.

For example, when using replacement experiments that test one material such as a FP in a fuel matrix, a bias between measured and calculated  $k_{eff}$  values for each state may be calculated. The difference in the bias between the two states is due primarily to any bias introduced by the test material. Figure 35 shows some of the key sensitivity information for three configurations from LEU-COMP-THERM-079, the  $^{103}\text{Rh}$  foil critical experiments performed at Sandia National Laboratories. Cases 002, 003, and 005, shown in Figure 35 have no  $^{103}\text{Rh}$ , 25-micron-thick foils and 100-micron-thick foils, respectively. Notice that the  $^{235}\text{U}$  fission and  $^{238}\text{U}$  n, $\gamma$  sensitivity profiles are very similar for all three configurations, even Case 002 with no  $^{103}\text{Rh}$ . Thus, one would expect the biases related to these reactions to be the same for all three systems. The  $k_{eff}$  value for each of the systems responds to the same nuclear data errors in the same way. The  $^{103}\text{Rh}$  n, $\gamma$  sensitivity profiles for Cases 3 and 5 shown in Figure 35 are small compared to the sensitivities for the primary nuclear reactions in these systems. As was discussed earlier, the experimental series is not similar to a spent fuel system and an overall bias calculated from this system is not applicable to a spent fuel system. It also is not clear that, if one could extract a  $^{103}\text{Rh}$  bias from these critical configurations, it would be applicable to a spent fuel system. The TSAR analysis technique coupled together with the TSURFER data adjustment technique does provide an estimate of a  $^{103}\text{Rh}$  bias that would be applicable to a spent fuel system.

Figure 36 shows some key reactivity sensitivity data profiles computed by TSAR between Cases 002 and 005, which have no  $^{103}\text{Rh}$  and 100-micron-thick foils, respectively.

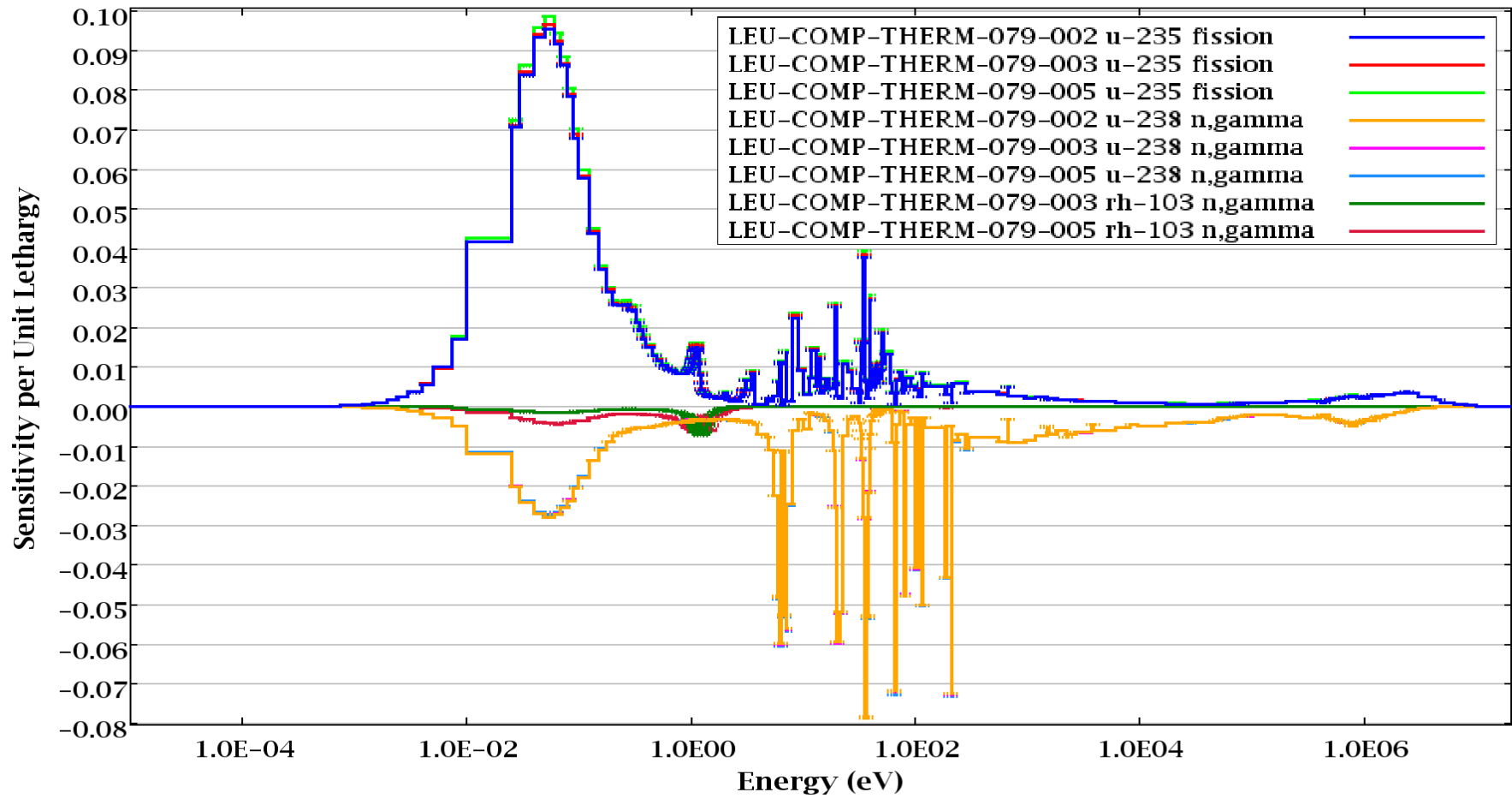


Figure 35.  $k_{eff}$  Sensitivity Profiles for Some Key Nuclear Reactions

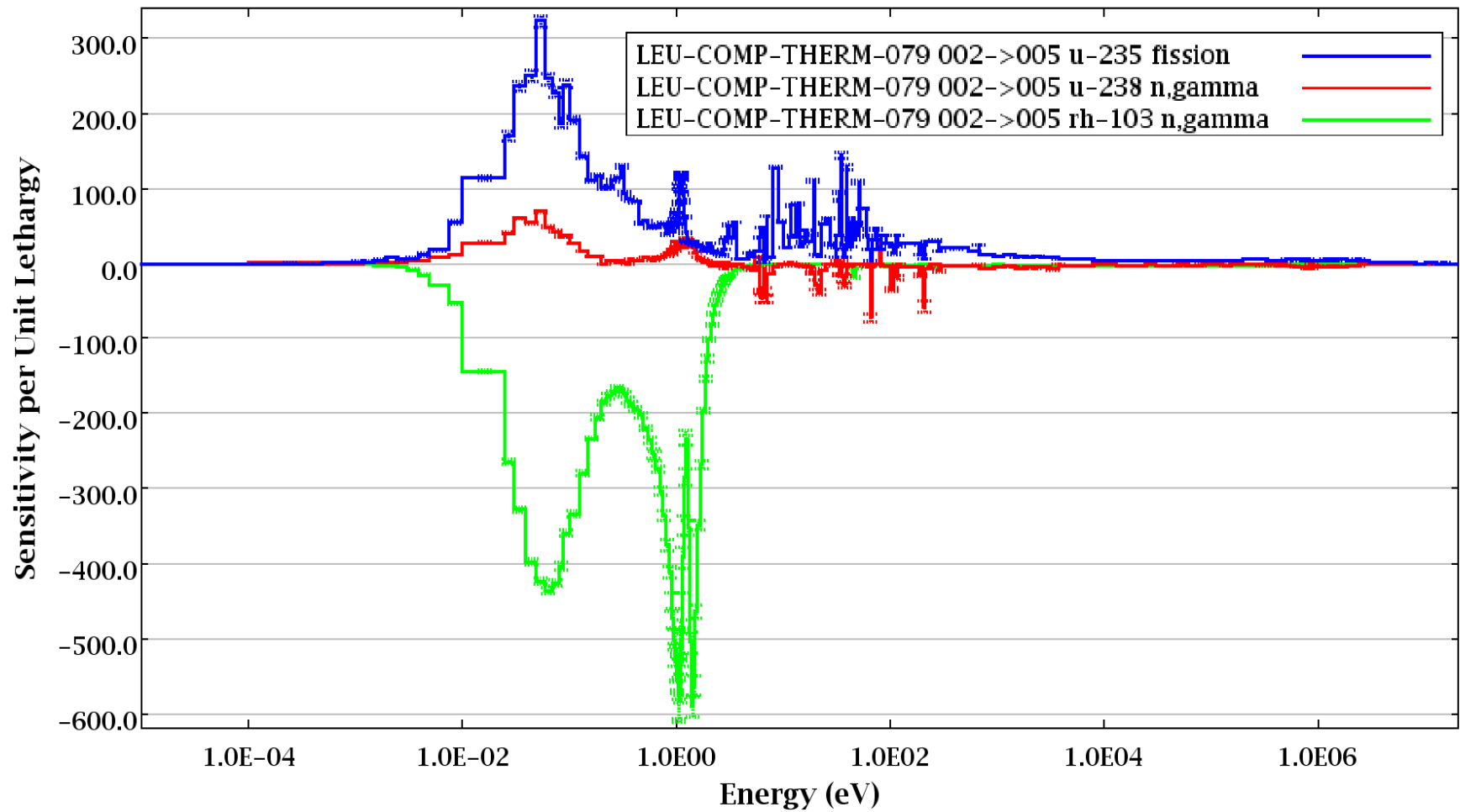


Figure 36. Reactivity Sensitivity ( $\text{pcm}/(\Delta\sigma/\sigma)$ ) Profiles for Some Key Nuclear Reactions

Use of the TSAR program has essentially discarded the sensitivities that are common to both Cases 002 and 005, retaining only the differences. Note the change in importance of the  $^{103}\text{Rh}$  n, $\gamma$  between Figures 35 and 36 relative to the  $^{235}\text{U}$  and  $^{238}\text{U}$  sensitivities. Inspection of Figure 36 shows that some of the reactivity bias would likely be due to errors in the thermal  $^{235}\text{U}$  fission cross sections. Ideally, if the critical experiments or reactivity oscillation experiments were crafted carefully enough, the only remaining sensitivity would be the target material. Thus any bias between measured and calculated reactivity would be due to the target material. However, if additional experiments that validate common materials such as  $^{235}\text{U}$  and  $^{238}\text{U}$  are included in the TSURFER analysis, these common nuclides will be adjusted and constrained by many other experiments, facilitating adjustments of data emphasized in the TSAR sensitivities.

Even the less than perfect reactivity sensitivity data generated for LEU-COMP-THERM-079 Cases 002 and 005 can be analyzed with the TSURFER data adjustment program to estimate the likely cross-section adjustments needed to adjust the calculated reactivity to match the measured reactivity, within its measurement uncertainty. The SA model  $k_{eff}$  sensitivity profiles can also be used in the same calculation to project the impact of the cross-section adjustments onto the SA model, thereby providing an estimate of the bias due solely to the FP.

It may be possible to apply the TSAR/TSURFER analysis technique to the MINERVE and DIMPLE FP oscillation experiments. The MINERVE and DIMPLE data are not currently available for evaluation using these techniques. Additional discussions and theoretical development of these techniques are provided in Ref. 31.

## CONCLUSIONS

Burnup credit, credit taken in the SA for the reduction in reactivity of nuclear fuel that occurs during use in a power reactor, is being utilized in the U.S. to maximize limited spent nuclear fuel storage and transportation capability. Particularly in transportation activities, the paucity of measured data suitable for use in validation of criticality calculations involving FPs has been an impediment to implementation of full burnup credit.

The work reported in this paper used sensitivity analysis to develop an understanding of how nuclear data variation affects the SA model  $k_{eff}$  value and explored the potential combination of  $k_{eff}$  sensitivity data and cross-section uncertainty data to produce estimates for the uncertainty in  $k_{eff}$  due to nuclear data uncertainties for a representative SA model. From this analysis, it is unlikely that the bias associated with the 16 FPs evaluated would be as large as 0.13%  $\Delta k/k$ , which is less than 2% of the FP worth from the model.

International Workshop on Advances in Applications of Burnup Credit for Spent Fuel Storage, Transport, Reprocessing, and Disposition, Cordoba, Spain, October 2009

The paper includes a review of measured data that might be useful for validation of FP burnup credit criticality calculations. For varying reasons, the available data is judged to be of limited usefulness for conventional bias determination techniques.

This paper also presented the application of generalized linear least-squares (e.g. TSURFER) and reactivity sensitivity and uncertainty analysis (e.g., TSAR/TSURFER) methods to the validation of FP burnup credit calculations. Application of such techniques to the available FP critical experiment data may yield improved estimates of bias and bias uncertainty associated with FPs in SA models.

## REFERENCES

- 1 J. C. Wagner, C. V. Parks, D. E. Mueller, "Assessment of benefits for extended burnup credit in transporting PWR spent nuclear fuel in the United States of America," *Advances in Applications of Burnup Credit to Enhance Spent Fuel Transportation, Storage, Reprocessing and Disposition*, Proceedings of a Technical Meeting held in London, 29 August–2 September 2005, IAEA-TECDOC-1547, International Atomic Energy Agency (May 2007).
- 2 C. V. Parks, J. C. Wagner, D. E. Mueller, and I. C. Gauld, "Full Burnup Credit in Transport and Storage Casks--Benefits and Implementation," *Radwaste Solutions* **14**(2), 32–41 (March/April 2007).
- 3 J. C. Wagner and D. E. Mueller, "Updated Evaluation of Burnup Credit for Accommodating PWR Spent Nuclear Fuel in High-Capacity Cask Designs," presented at the 2005 NCSD Topical Meeting, Knoxville, TN, September 19–22, 2005.
- 4 C. V. Parks and J. C. Wagner, "Current Status and Potential Benefits of Burnup Credit for Spent Fuel Transportation," Proc. of American Nuclear Society, 14th Pacific Basin Conf., Honolulu, Hawaii, March 21-25, 2004.
- 5 T. L. Sanders and R. M. Westfall, "Feasibility and Incentives for Burnup Credit in Spent Fuel Transport Casks," *Nucl. Sci. Eng.* **104**, 66–77 (1990).
- 6 W. A. Boyd and G. N. Wrights, "Past Experience and Future Needs for the Use of Burnup Credit in LWR Fuel Storage," *Trans. Am. Nucl. Soc.* **55**, 396 (1987).
- 7 T. L. Sanders, R. M. Westfall, and R. H. Jones, *Feasibility and Incentives for the Consideration of Spent Fuel Operating Histories in the Criticality Analysis of Spent Fuel Shipping Casks*, SAND87-0151, TTC-0713, UC-71, Sandia National Laboratory (August 1987).
- 8 "Validation of Neutron Transport Methods for Nuclear Criticality Safety Calculations," ANSI/ANS-8.24-2007, an American National Standard, published by the American Nuclear Society, LaGrange Park, IL, 2007.
- 9 "Burnup Credit for LWR Fuel," ANSI/ANS-8.27-2008, an American National Standard, published by the American Nuclear Society, LaGrange Park, IL, 2008.
- 10 *SCALE: A Modular Code System for Performing Standardized Computer Analyses for Licensing Evaluations*, ORNL/TM-2005/39, Version 6, Vols. I–III (January 2009). Available from Radiation Safety Information Computational Center at Oak Ridge National Laboratory as CCC-750.

- 11 J. C. Wagner, *Computational Benchmark for Estimation of Reactivity Margin from Fission Products and Minor Actinides in PWR Burnup Credit*, NUREG/CR-6747 (ORNL/TM-2000/306), U.S. Nuclear Regulatory Commission, Oak Ridge National Laboratory, October 2001.
- 12 “Nuclear Fuel Data,” Form RW-859, Energy Information Administration, 2004. This document included U.S. spent fuel inventory data through the end of 2002.
- 13 B. L. Broadhead, B. T. Rearden, C. M. Hopper, J. J. Wagschal, and C. V. Parks, *Sensitivity- and Uncertainty-Based Criticality Safety Validation Techniques*, Nucl. Sci. Eng. **146**, 340-366 (2004).
- 14 F. Fernex, “Programme HTC – Phase 1: Réseaux de crayons dans l’eau pure (Water-moderated and reflected simple arrays) Réévaluation des expériences,” DSU/SEC/T/2005-33/D.R., Institut de Radioprotection et de Sûreté Nucléaire, 2008.
- 15 F. Fernex, “Programme HTC – Phase 2: Réseaux simples en eau empoisonnée (bore et gadolinium)(Reflected simple arrays moderated by poisoned water with gadolinium or boron) Réévaluation des expériences,” DSU/SEC/T/2005-38/D.R., Institut de Radioprotection et de Sûreté Nucléaire, 2008.
- 16 F. Fernex, “Programme HTC – Phase 3: Configurations ‘stockage en piscine’ (Pool storage) Réévaluation des expériences,” DSU/SEC/T/2005-37/D.R., Institut de Radioprotection et de Sûreté Nucléaire, 2008.
- 17 F. Fernex, “Programme HTC – Phase 4: Configurations ‘châteaux de transport’ (Shipping cask) - Réévaluation des expériences,” DSU/SEC/T/2005-36/D.R., Institut de Radioprotection et de Sûreté Nucléaire, 2008.
- 18 *International Handbook of Evaluated Criticality Safety Benchmark Experiments*, NEA/NSC/DOC(95)03, NEA Nuclear Science Committee, September 2009.
- 19 D. E. Mueller, K. R. Elam, and P. B. Fox, *Evaluation of the French Haut Taux de Combustion (HTC) Critical Experiment Data*, NUREG/CR-6979 (ORNL/TM-2007/083), prepared for the U.S. Nuclear Regulatory Commission by Oak Ridge National Laboratory, Oak Ridge, Tenn., September 2008.
- 20 N. Leclaire, T. Ivanova, E. Létang, E. Girault, and J. Thro, “Fission Product Experimental Program: Validation and Computational Analysis,” *Nuc. Sci. and Eng.* **161**, 188–215 (2009).
- 21 D. E. Mueller and G. A. Harms, “Using the SCALE 5 TSUNAMI-3D Sequence in Critical Experiment Design,” *Trans. Am. Nucl. Soc.* **93**, 263–266 (2005).

- 22 P. Baeten, P. D'hondt, L. Sannen, D. Marloye (BN), B. Lance (BN), A. Renard (BN), and J. Basselier (BN), "The REBUS-PWR Experimental Programme for Burn-up Credit," Integrating Criticality Safety into the Resurgence of Nuclear Power, Knoxville, Tennessee, September 19–22, 2005, on CD-ROM, American Nuclear Society, LaGrange Park, IL (2005).
- 23 M. Hennebach and H. Kuhl, "Monte Carlo Calculations of the REBUS Critical Experiment for Validation of Burnup Credit," presented at the *IAEA Technical Meeting on Burnup Credit*, London, August 29, 2005.
- 24 A. Santamarina, "From Integral Experiments to Nuclear Data Improvement," invited paper presented at the *International Conference on Nuclear Data for Science and Technology 2007*, Nice, France, 2007.
- 25 C. J. Dean, P. J. Smith, and R. J. Perry, "Validation of Important Fission Product Evaluations through CERES Integral Benchmarks," paper presented at the *International Conference on Nuclear Data for Science and Technology 2007*, Nice, France, 2007.
- 26 A. Santamarina et al., "Experimental Validation of Burnup Credit Calculations by Reactivity Worth Measurements in the Minerve Reactor," Proc. of Fifth International Conference on Nuclear Criticality Safety, Albuquerque, NM, September 1995.
- 27 P. J. Finck, R. N. Blomquist, C. G. Stenberg, and C. Jammes, *Evaluation of Fission Product Worth Margins in PWR Spent Nuclear Fuel Burnup Credit Calculations*, ANL-FRA-1998-1, Argonne National Laboratory, February 1999.
- 28 G. Radulescu, D. E. Mueller, and J. C. Wagner, *Sensitivity and Uncertainty Analysis of Commercial Reactor Criticals for Burnup Credit*, NUREG/CR-6951 (ORNL/TM-2006/87), prepared for the U.S. Nuclear Regulatory Commission by Oak Ridge National Laboratory, Oak Ridge, Tenn., December 2007.
- 29 J. A. Roberts, "Further Interpretation of Sensitivity Data in Support of Burnup Credit," M.S. Thesis, University of Wisconsin – Madison, August 2009.
- 30 M. L. Williams, "Sensitivity and Uncertainty Analysis for Eigenvalue-Difference Responses," *Nucl. Sci. Eng.* **155**(1), 18–36 (January 2007).
- 31 B. T. Rearden, M. L. Williams, M. A. Jessee, D. E. Mueller and D. A. Wiarda, "TSUNAMI Sensitivity and Uncertainty Analysis Capabilities and Data," submitted for publication to *Nucl. Tech.*, (2009).